Available online at http://scik.org
Commun. Math. Biol. Neurosci. 2023, 2023:134
https://doi.org/10.28919/cmbn/8319
ISSN: 2052-2541

DYNAMICAL BEHAVIOR AND SENSITIVITY ANALYSIS OF A DENGUE REINFECTION MODEL FOR VERTICAL TRANSMISSION INCORPORATING MULTIPLE CONTROL STRATEGIES

R. PREM KUMAR[1,2], G.S. MAHAPATRA[1], RANA D. PARSHAD[3,*], P.K. SANTRA[4]

[1]Department of Mathematics, National Institute of Technology Puducherry, Karaikal-609609, India

[2]Department of Mathematics, Avvaiyar Government College for Women, Karaikal-609602, Puducherry, India

[3]Department of Mathematics, Iowa State University, Ames, IA 50011, USA

[4]Moulana Abul Kalam Azad University of Technology, Kolkata–700064, India

Abstract. The dynamics of dengue disease with reinfection and three control techniques are proposed in this research. The epidemic model includes a saturated incident function in virus transmission among humans. The vertical transmission of the virus in vectors and a reinfection scenario in the human population are added to the proposed dengue epidemic model. In relation to the basic reproduction number R_0, the existence and stability of the equilibrium points of the proposed epidemic model are studied. The equilibrium states of the epidemic model are examined for both local and global stability. For the basic reproduction number R_0, a sensitivity analysis is carried out in relation to various parameters. Bifurcation analysis is performed for the proposed model, and the bifurcation parameter is identified. In the proposed dengue epidemic model, we introduce three time-dependent controls: protection control, treatment control, and insecticide spray control. In the proposed model, a control problem is identified and analytically solved. The conditions for the optimal control strategies for the control problem are derived using Pontryagin's maximal principle. In order to demonstrate the effectiveness of the control measures, numerical simulations are used. Finally, suggestions for preventing the spread of the dengue virus are presented.

*Corresponding author

E-mail address: rparshad@iastate.edu

Received November 04, 2023

Keywords: dengue virus; vertical transmission; reinfection; stability; sensitivity; bifurcation.

2020 AMS Subject Classification: 92C60.

1. INTRODUCTION

Humans who are bitten by dengue infected mosquitoes contract the dengue virus. Aedes aegypti mosquitoes and, to a lesser extent, Ae. albopictus mosquitoes are primarily responsible for the disease's transmission. Dengue virus is the name of the virus that causes dengue (DENV). There are four different DENV serotypes, and there can be a maximum of four infections caused by each virus. Severe dengue is the primary cause of illness and death in many Asian and Latin American nations. It needs to be managed by health professionals. A specific treatment is not available for dengue or severe dengue. Death rates from severe dengue are reduced to about 1% when disease progression is identified early and patients have access to quality medical care. Dengue is a tropical and subtropical disease that mostly affects urban and semi-urban regions. About half of the world's population is now at risk due to the rapid increase in dengue incidence worldwide.Although it's estimated that between 100 and 400 million illnesses happen each year, more than 80% of them are typically mild and asymptomatic. For the prevention and management of dengue, effective vector control techniques are crucial. Long-term community involvement can significantly enhance vector control efforts. DENV can cause a severe flu-like illness, but most people who get it only feel moderately sick. This can occasionally progress to severe dengue, a potentially fatal consequence [1]. In various tropical regions of the world, dengue fever, a viral disease spread by mosquitoes, has returned in a significant way because the disease's severe form results in a lot of illness and death [2]. In the realm of epidemiological research, understanding and modeling the dynamics of infectious diseases is of paramount importance. The global burden of diseases like dengue fever necessitates the development of intricate models that can provide insights into the factors driving their spread. This comprehensive review delves into a myriad of dengue epidemic models and their variants, each designed to capture specific aspects of the disease's behavior and transmission patterns.

These models span a spectrum of complexities, taking into account various factors that influence dengue transmission dynamics. Notable among them are the models that tackle general dengue epidemics [3, 4, 5, 6, 7, 8, 9, 10, 11, 12, 13, 14, 15, 16, 17, 18, 19, 20], which form the

foundation for understanding the overall spread of the disease. Going beyond the basics, researchers have explored dengue models with relapse [21], examining the potential for recurrent infections.

A significant branch of research involves optimizing control strategies, leading to dengue models with optimal control [22, 23, 24, 25, 26, 27, 28, 29, 30, 31, 32]. These models aim to identify interventions that could effectively curb the disease's impact. Additionally, researchers have examined the influence of pulse and periodic behaviors on dengue dynamics [33], adding an element of temporal variability to the models.

The evolution of dengue doesn't unfold in isolation, and the interaction between different strains adds complexity to the scenario. Multi-strain dengue models [34, 35, 36, 37, 38, 39, 40, 41] consider the coexistence and competition among multiple dengue strains. Temperature and climate effects are also crucial factors affecting dengue transmission, and models have been developed to incorporate these [42, 43, 44].

Innovative approaches to disease control are explored in dengue models with Wolbachia bacterium controls [45, 46, 47, 48], seeking to harness biological methods to limit transmission. Furthermore, dengue models accommodating seasonal variations in vector population [49, 50] provide insights into the disease's behavior under changing ecological conditions.

Given the pressing need for effective preventive measures, dengue models with vaccine strategies [51, 52] delve into understanding the potential impact of vaccination campaigns. The dynamics of sequential transmission [53] and the influence of age of infection [54] on disease outcomes have also been analyzed.

Considering the interplay between dengue and the immune system, models exploring secondary dengue infections [55, 56] and reinfections with the same serotype [57] contribute to a deeper comprehension of immunity patterns. Moreover, the role of treatment in controlling the disease has been examined in certain models [58]. Real-world factors, such as human movements, have a substantial impact on disease spread. Dengue models accounting for human mobility [59] provide insights into how population movements can influence transmission dynamics. The influence of age structure [60, 61] have also been investigated to understand their

implications on dengue transmission.

Vertical Transmission in existing Dengue models:

In recent years, several research papers have focused on the mathematical modeling of vertical transmission of dengue transmission among vectors, providing insights into the role of this mode of transmission in dengue dynamics [62, 63]. Several studies have focused on the role of vertical transmission, which occurs when the virus is transmitted from infected female mosquitoes to their offspring. Vertical transmission refers to the transmission of a pathogen from an infected female mosquito to her offspring [64]. In the case of dengue, vertical transmission can occur in Aedes mosquitoes, such as *Aedes aegypti* and *Aedes albopictus*. Infected female mosquitoes can pass the dengue virus to their eggs, resulting in infected larvae and subsequent infected adult mosquitoes. This mechanism of transmission has significant implications for the persistence and spread of dengue within mosquito populations.

Dengue Transmission: Research Gaps and Analysis:

Research on modeling and analysing a dengue transmission model incorporating vertical transmission, non-monotonic incident function, bifurcation, optimal control, sensitivity, and numerical analysis is severely limited. Despite the significance of these factors in understanding and controlling the spread of dengue, there remains a scarcity of comprehensive studies encompassing all these aspects. Vertical transmission, which involves the dengue virus transmission from infected mother mosquitoes to their offspring, has been identified as a crucial factor in dengue dynamics. Additionally, incorporating non-monotonic incident functions [65] accounts for the nonlinear relationship between the mosquito population and the transmission rate. Bifurcation analysis aids in identifying critical thresholds and transitions in the system's behavior. Optimal control strategies enable the development of effective interventions to mitigate dengue transmission [66]. Sensitivity and numerical analysis provide insights into the robustness and accuracy of the model [67]. Given the limited research in this area, further investigations are necessary to enhance our understanding of dengue dynamics and facilitate the development of targeted control measures. In this comprehensive review, we embark on a journey through a multitude of dengue epidemic models and their diverse adaptations. Each model represents a

unique perspective on understanding the complex interplay of factors governing dengue transmission, offering valuable insights for public health interventions and policies moving forward. Analyzing the dynamics of dengue virus transmission and developing the most effective preventative measures are the main goals of this research. The model incorporates a non-monotonic incident function for disease transmission among the susceptible host population. In the model, vertical virus transmission among vectors is studied. The reinfection of the human population after its recovery is well studied. The vector population is subdivided into adult and egg populations. Following a study of the model's dynamical analysis, a model with optimum control taking into account the effective controls for the eradication of the dengue virus is investigated.

We offer a brief literature overview of the numerous mathematical models that relate to the spread of the dengue virus among humans in this section. The remainder of the paper is structured as follows: In section (2), the model's formulation and a description of its various parameters are covered. The fundamental characteristics of the model are described in Section (3). In Section (4), the model's stationary points, existence, and fundamental reproduction number are presented. Section (5) discusses the stability analysis of the system at the equilibrium points. Sections (6) and (7), respectively, present the model's sensitivity and bifurcation analyses. The optimal control analysis of the control problem is covered in Section (8). The numerical analysis is covered in Section (9). Finally, Section (10) summarises all the research results.

2. Conceptualization of Dengue Reinfection Model

A deterministic mathematical model with the vertical transmission in vectors with reinfection is formulated with a transfer diagram given in figure (1). The saturated incident function in human transmission is used while formulating the model. $\rho(1-c_1)\alpha_1 I_m$ measures the infection force of the disease and $\frac{1}{1+kI_m}$ measures the inhibition effect from the behavioral change of the susceptible individuals when their number increases. The function $\frac{\rho(1-c_1)\alpha_1 I_m}{1+kI_m}$ tends to a saturation level when I_m, the infected vector population at any time t gets large [68, 69]. The four classes that make up the entire human population are: the susceptible human class ($S_h(t)$), the exposed human class ($E_h(t)$), the infected human class ($I_h(t)$), and the recovered human class ($R_h(t)$). The entire adult mosquito population is classified into three classes: susceptible mosquitoes class ($S_m(t)$), exposed mosquitoes class ($E_m(t)$), and infected mosquitoes class

($I_m(t)$). Infected eggs class ($I_e(t)$ and susceptible eggs class ($S_e(t)$) comprise the two classes that make up the total population of mosquito eggs. The life stages of a mosquito say egg, larva, and pupa are termed in this model as egg population. The following assumptions govern the development of the mathematical model: (i) It is considered that the recruitment rate of mosquito egg population and susceptible humans are constant. (ii) For both human and mosquito populations, the natural death rates are taken into account. (iii) When infected adult mosquitoes bite susceptible humans, a horizontal virus infection from the infected mosquitoes to the susceptible human occurs. The transmission coefficient is $\frac{\rho(1-c_1)\alpha_1 I_m S_h}{1+kI_m}$. (iv) When the susceptible adult mosquitoes bite the infected person, the infected human transmits the virus horizontally to the susceptible adult mosquitoes, and the transmission coefficient is provided by $\rho(1-c_1)\alpha_2 I_h S_m$. (v) The humans recovered from dengue disease can be susceptible to the same serotype dengue virus [70], and the transmission coefficient is given by δR_h. Tables (1), (3), and (2) provide descriptions of the various state variables, control variables, and system parameters, respectively.

$$
\left\{
\begin{array}{ll}
\frac{dS_h}{dt} & = \Omega - \frac{\rho(1-c_1)\alpha_1 I_m S_h}{1+kI_m} - \mu S_h + \delta R_h \\
\frac{dE_h}{dt} & = \frac{\rho(1-c_1)\alpha_1 I_m S_h}{1+kI_m} - (\beta_1 + \mu) E_h \\
\frac{dI_h}{dt} & = \beta_1 E_h - (\gamma + d + \mu + bc_2) I_h \\
\frac{dR_h}{dt} & = (\gamma + bc_2) I_h - (\delta + \mu) R_h \\
\frac{dS_m}{dt} & = \phi S_e - \rho(1-c_1)\alpha_2 I_h S_m - (\xi + pc_3) S_m \\
\frac{dE_m}{dt} & = \rho(1-c_1)\alpha_2 I_h S_m - (\beta_2 + \xi + pc_3) E_m \\
\frac{dI_m}{dt} & = \beta_2 E_m + \phi I_e - (\xi + pc_3) I_m \\
\frac{dS_e}{dt} & = \Psi - \theta\pi I_m - (\phi + pc_3) S_e \\
\frac{dI_e}{dt} & = \theta\pi I_m - (\phi + pc_3) I_e
\end{array}
\right. \tag{1}
$$

The preliminary condition is

$$
S_h > 0, E_h \geq 0, I_h \geq 0, R_h \geq 0, S_m > 0, E_m \geq 0, I_m \geq 0, S_e > 0, I_e \geq 0. \tag{2}
$$

TABLE 1. Description of the state variables of the model-(1) of dengue transmission.

State variable	Description of populations at a time t.
$S_h(t)$	Number of the susceptible human population.
$E_h(t)$	Number of the exposed human population.
$I_h(t)$	Number of dengue virus-infected human population.
$R_h(t)$	Number of recovered human population from the dengue infection.
$S_m(t)$	Number of susceptible mosquito population.
$E_m(t)$	Number of exposed mosquito population.
$I_m(t)$	Number of dengue virus-infected mosquito population.
$S_e(t)$	Number of susceptible egg population.
$I_e(t)$	Number of infected egg population.

TABLE 2. An overview of the parameters of the dengue transmission model-(1).

Parameter	Description
Ω	Human population recruitment rate.
α_1, α_2	Rate of disease transmission within human and mosquito populations, respectively.
β_1, β_2	Progression rate from exposed to infected human and mosquito population, respectively.
μ, ξ	Natural death rate for human and mosquito population, respectively.
δ	The rate at which the recovered humans become susceptible.
d	The disease induced mortality rate of humans.
k	Saturation factor.
γ	The natural recovery rate of humans.
b, p	Effectiveness of the control c_2 and c_3, respectively.
ϕ	The development rate of Aedes Aegypti mosquitoes.
θ	The total number of Aedes Aegypti mosquitoes eggs laid per mosquito in lifetime.
π	The vertical transmission rate of Aedes Aegypti mosquitoes.
Ψ	Recruitment rate of Aedes Aegypti mosquitoes eggs per day.

TABLE 3. Description of three control parameters of the system (1)

Control Parameter	Description
c_1	Protection controls like the use of bednets, mosquito repellent creams, etc.
c_2	Treatment control for humans infected with either of the serotype viruses.
c_3	Insecticide spray control against mosquitoes.

The effective biting rate of female Aedes Aegypti mosquitoes is $\rho=\chi\zeta\eta$, where χ is the number of bites per human in a given amount of time, ζ is the proportion of infected bites that resulted in infection, and η is the ratio of mosquito counts to human numbers.

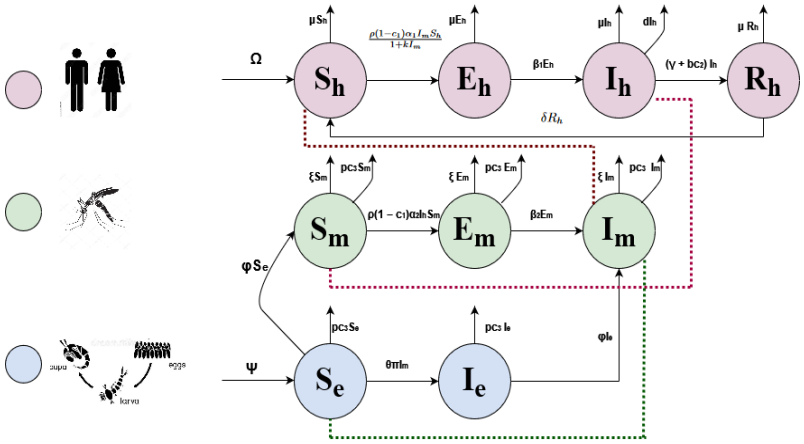

FIGURE 1. Dengue virus transmission diagram has three populations, namely the human population, the adult Aedes aegypti mosquito population, and the egg population.

3. PRIMARY CHARACTERISTICS OF PROPOSED DENGUE REINFECTION MODEL

The positivity and uniform boundedness of the system(1) solution with initial condition (2) are examined in this part, along with the determination of the positively invariant region for the system (1) solutions.

3.1. Non-negativity property in solutions of Dengue reinfection model.

The non-negativity characteristic of solutions of the model (1) is shown in this subsection.

Theorem 1. *For each $t > 0$, the solution trajectories of the system (1) with the preliminaries conditions (2) are non-negative.*

Proof. Let us assume that $f_1 = \beta_1 + \mu, f_2 = \gamma + d + \mu + bc_2, f_3 = \gamma + bc_2, f_4 = \delta + \mu, f_5 = \xi + pc_3, f_6 = \beta_2 + \xi + pc_3, f_7 = \phi + pc_3$. From the first equation of the system (1) using the preliminary condition $S_h(0) > 0$, we get $\dot{S_h} = \Omega - \left(\frac{\rho(1-c_1)\alpha_1 I_m S_h}{1+kI_m} + \mu S_h\right) + \delta R_h > -\left(\frac{\rho(1-c_1)\alpha_1 I_m}{1+kI_m} + \mu\right) S_h$ and hence $\frac{dS_h}{S_h} > -\left(\frac{\rho(1-c_1)\alpha_1 I_m}{1+kI_m} + \mu\right) dt$. After integrating, we get

$S_h(t) > S_h(0)e^{-\int_0^t \left[\frac{\rho(1-c_1)\alpha_1 I_m}{1+kI_m}+\mu\right]dt} > 0$ for $t > 0$. Using the second equation of system (1), we get $\dot{E_h} = \frac{\rho(1-c_1)\alpha_1 I_m S_h}{1+kI_m} - f_1 E_h \geq -f_1 E_h$ and $\frac{dE_h}{E_h} \geq -f_1 dt$. Hence $E_h(t) \geq E_h(0)e^{-\int_0^t f_1 dt} = E_h(0)e^{-f_1 t} \geq 0$ for all $t > 0$. Similarly from other equations of the system (1) with preliminary condition (2), we get $I_h(t) \geq I_h(0)e^{-\int_0^t f_2 dt} = I_h(0)e^{-f_2 t}$, $R_h(t) \geq R_h(0)e^{-\int_0^t f_4 dt} = R_h(0)e^{-f_4 t}$, $S_m(t) \geq S_m(0)e^{-\int_0^t (\rho(1-c_1)\alpha_2 I_m + f_5)dt} > 0$, $E_m(t) \geq E_m(0)e^{-f_6 t} \geq 0$, $I_m(t) \geq I_m(0)e^{-f_5 t} \geq 0$, $S_e > S_e(0)e^{-f_7 t} > 0$, $I_e(t) \geq I_e(0)e^{-f_7 t} \geq 0$. Hence solutions of the system (1) with preliminary conditions (2) are non-negative for $t > 0$. □

3.2. Uniform boundedness of the solutions of Dengue reinfection model.

Theorem 2. *All solutions of the system (1) with preliminary conditions (2) are uniformly bounded in the region* $\Theta = \{(S_h, E_h, I_h, R_h, S_m, E_m, I_m, S_e, I_e) \in \mathbb{R}^9_+ | 0 < N(t) \leq \frac{\Omega+\Psi}{m}\}$.

Proof. Let $N_h(t)$, $N_m(t)$, and $N_e(t)$ represent the total humans, adult Aedes Aegypti mosquitoes, Aedes Aegypti egg population respectively. Suppose $N(t)$ represents the entire population at any time t. Hence

$$\begin{aligned} \frac{dN}{dt} &= \dot{S_h} + \dot{E_h} + \dot{I_h} + \dot{R_h} + \dot{S_m} + \dot{E_m} + \dot{I_m} + \dot{S_e} + \dot{I_e} \\ &= \Omega - \mu(S_h + E_h + I_h + R_h) - dI_h - \xi(S_m + E_m + I_m) - pc_3(S_m + E_m + I_m) + \Psi - pc_3(S_e + I_e) \\ &= \Omega + \Psi - \mu N_h - dI_h - \xi N_m - pc_3 N_m - pc_3 N_e \end{aligned} \tag{3}$$

For $m = \min(\mu, \xi)$, we get

$$\begin{aligned} \frac{dN}{dt} + mN &= \Omega + \Psi - \mu N_h - dI_h - \xi N_m - pc_3 N_m - pc_3 N_e + m(N_h + N_m + N_e) \\ &\leq \Omega + \Psi - (\mu - m)N_h - (\xi - m)N_m \\ &\leq \Omega + \Psi \end{aligned} \tag{4}$$

Hence

$$\frac{dN}{dt} + mN \leq \Omega + \Psi \tag{5}$$

By applying the theory of Differential inequality,

$$0 < N(t) \leq \frac{\Omega + \Psi}{m}(1 - e^{-mt}) + N(0)e^{-mt} \tag{6}$$

as $t \to \infty$, we get

$$0 < N(t) \leq \frac{\Omega + \Psi}{m} \tag{7}$$

Thus every solution of the system (1) with preliminary conditions (2) which initiate in $\mathbb{R}^9_+$ are uniformly bounded and are restricted inside $\Theta = \{(S_h, E_h, I_h, R_h, S_m, E_m, I_m, S_e, I_e) \in \mathbb{R}^9_+ : 0 < N(t) \leq \frac{\Omega+\Psi}{m}, m = \min(\mu, \xi)\}$ □

4. Stationary Points and Their Existence of the Dengue Model

The system (1) has two equilibrium points, which are as follows: a disease-free equilibrium (DFE) Q_0 and a unique endemic equilibrium (EE) Q_1:

(1) The disease-free equilibrium (DFE) point is $Q_0 = (S_h^0, E_h^0, I_h^0, R_h^0, S_m^0, E_m^0, I_m^0, S_e^0, I_e^0)$, where $S_h^0 = \frac{\Omega}{\mu} > 0$, $E_h^0 = 0$, $I_h^0 = 0$, $R_h^0 = 0$, $S_m^0 = \frac{\phi\Psi}{f_5 f_7} > 0$, $E_m^0 = 0$, $I_m^0 = 0$, $S_e^0 = \frac{\Psi}{f_7} > 0$, $I_e^0 = 0$.

(2) The endemic equilibrium (EE) point is $Q_1 = (S_h^*, E_h^*, I_h^*, R_h^*, S_m^*, E_m^*, I_m^*, S_e^*, I_e^*)$, where
$S_h^* = \frac{f_1 f_2 f_5 f_6 (1+kI_m)(f_5 f_7 - \pi\theta\pi)}{(1-c_1)^2 \alpha_1 \alpha_2 \beta_1 \rho^2 (f_6 \pi\theta\phi - f_5 f_6 f_7 - \pi\beta_2\theta\phi) I_m + \beta_2 \phi \Psi} > 0$,
$I_h^* = \frac{f_5 f_6 (f_5 f_7 - \pi\theta\phi) I_m}{(1-c_1)\alpha_2 \rho (f_6 \pi\theta\phi - f_5 f_6 f_7 - \pi\beta_2\theta\phi) I_m + \beta_2 \phi \Psi} > 0$,
$E_h^* = \frac{f_2 f_5 f_6 (f_5 f_7 - \pi\theta\phi) I_m}{(1-c_1)\alpha_2 \beta_1 \rho (f_6 \pi\theta\phi - f_5 f_6 f_7 - \pi\beta_2\theta\phi) I_m + \beta_2 \phi \Psi} > 0$,
$R_h^* = \frac{f_3 f_5 f_6 (f_5 f_7 - \pi\theta\phi) I_m}{(1-c_1) f_4 \alpha_2 \rho (f_6 \pi\theta\phi - f_5 f_6 f_7 - \pi\beta_2\theta\phi) I_m + \beta_2 \phi \Psi} > 0$, $S_m^* = \frac{(f_6 \pi\theta\phi - f_5 f_6 f_7 - \pi\beta_2\theta\phi) I_m + \beta_2 \phi \Psi}{f_5 f_7 \beta_2} > 0$, $E_m^* = \frac{(f_5 f_7 - \theta\pi\phi) I_m}{f_7 \beta_2} > 0$, $S_e^* = \frac{\Psi - \pi\theta I_m}{f_7} > 0$, $I_e^* = \frac{\pi\theta I_m}{f_7} > 0$.
Here $f_1 = \beta_1 + \mu, f_2 = \gamma + d + \mu + bc_2, f_3 = \gamma + bc_2, f_4 = \delta + \mu, f_5 = \xi + pc_3, f_6 = \beta_2 + \xi + pc_3, f_7 = \phi + pc_3$. We assume that $f_5 f_7 - \pi\theta\phi > 0$.
Obviously, $(f_6 \pi\theta\phi - f_5 f_6 f_7 - \pi\beta_2\theta\phi) I_m + \beta_2 \phi \Psi > 0$ if and only if $0 < I_m < A$, where, $A = \frac{\beta_2 \phi \Psi}{f_6 (f_5 f_7 - \pi\theta\phi) + \pi\beta_2\theta\phi} > 0$. Hence $S_h^* > 0, E_h^* > 0, I_h^* > 0, R_h^* > 0, S_m^* > 0, E_m^* > 0, S_e^* > 0, I_e^* > 0$ if and only if $f_5 f_7 - \pi\theta\phi > 0$ and $0 < I_m < A$. Substituting the values of $S_h^*, E_h^*, I_h^*, R_h^*, S_m^*, E_m^*, S_e^*, I_e^*$ in the first equation of the system (1), a quadratic equation is obtained in I_m^* given by

$$A_1 I_m^{*2} + A_2 I_m^* + A_3 = 0 \tag{8}$$

where

$$
\begin{aligned}
A_1 &= f_5 f_6 k(f_1 f_2 f_4 k\mu + (1-c_1)\alpha_1(f_1 f_2 f_4 - f_3\beta_1\delta)\rho)(f_5 f_7 - \pi\theta\phi) \\
&\quad + (1-c_1)^2 f_4 k\alpha_1\alpha_2\beta_1\rho^2(f_5 f_6 f_7 + \pi(-f_6+\beta_2)\theta\phi)\Omega \\
A_2 &= f_5 f_6(2f_1 f_2 f_4 k\mu + (1-c_1)\alpha_1(f_1 f_2 f_4 - f_3\beta_1\delta)\rho)(f_5 f_7 - \pi\theta\phi) \\
&\quad + (1-c_1)^2 f_4\alpha_1\alpha_2\beta_1\rho^2(f_5 f_6 f_7 - \phi\ (\pi(f_6-\beta_2)\theta + k\beta_2\Psi))\Omega \\
A_3 &= f_1 f_2 f_4 f_5 f_6\mu(f_5 f_7 - \pi\theta\phi) - (1-c_1)^2 f_4\alpha_1\alpha_2\beta_1\beta_2\rho^2\phi\Psi\Omega \\
&= f_1 f_2 f_4 f_5 f_6\mu(f_5 f_7 - \pi\theta\phi)\left[1 - R_0^2\right]
\end{aligned} \tag{9}
$$

where

$$
R_0 = \sqrt{\frac{(1-c_1)^2\rho^2\alpha_1\alpha_2\beta_1\beta_2\phi\Psi\Omega}{f_1 f_2 f_5 f_6\mu(f_5 f_7 - \pi\theta\phi)}} \tag{10}
$$

called basic reproduction number (BRN) for the Dengue system (1) derived in the next section. Since $0 < I_m < A$, we get $A_1 > 0$ and $A_3 < 0$ if and only if $R_0 > 1$. Hence by the Descarte's rule of sign, equation (8) has exactly only a positive root. Hence Q_1 exists if $R_0 > 1$ in the region $\Upsilon = \{(S_h, E_h, I_h, R_h, S_m, E_m, I_m, S_e, I_e) \in \mathbb{R}_+^9 : 0 < N(t) \leq \frac{\Omega+\Psi}{m}, 0 < I_m < \min(A, \frac{\Omega+\Psi}{m}), m = \min(\mu, \xi)\}$

The BRN is the average number of secondary infections caused by a single infection. It's one of the most important threshold values for numerically representing the spread of a virus infection. At $Q = (S_h, E_h, I_h, R_h, S_m, E_m, I_m, S_e, I_e) \in \Upsilon$, the Jacobian matrix is given by $J(Q)$, where

(11)

$$
J(Q) = \begin{pmatrix}
-\frac{\rho(1-c_1)\alpha_1 I_m}{1+kI_m} - \mu & 0 & 0 & \delta & 0 & 0 & -\frac{\rho(1-c_1)\alpha_1 S_h}{(1+kI_m)^2} & 0 & 0 \\
\frac{\rho(1-c_1)\alpha_1 I_m}{1+kI_m} & -f_1 & 0 & 0 & 0 & 0 & \frac{\rho(1-c_1)\alpha_1 S_h}{(1+kI_m)^2} & 0 & 0 \\
0 & \beta_1 & -f_2 & 0 & 0 & 0 & 0 & 0 & 0 \\
0 & 0 & f_3 & -f_4 & 0 & 0 & 0 & 0 & 0 \\
0 & 0 & -\rho(1-c_1)\alpha_2 S_m & 0 & -(\rho(1-c_1)\alpha_2 I_h + f_5) & 0 & 0 & \phi & 0 \\
0 & 0 & \rho(1-c_1)\alpha_2 S_m & 0 & \rho(1-c_1)\alpha_2 I_h & -f_6 & 0 & 0 & 0 \\
0 & 0 & 0 & 0 & 0 & \beta_2 & -f_5 & 0 & \phi \\
0 & 0 & 0 & 0 & 0 & 0 & -\theta\pi & -f_7 & 0 \\
0 & 0 & 0 & 0 & 0 & 0 & \theta\pi & 0 & -f_7
\end{pmatrix}
$$

The asymptotic stability of Q_0 corresponds to eigenvalues of the characteristic equation of $J(Q_0)$ being of negative real parts, as confirmed by the computation of Basic reproduction number using the next-generation matrix approach. Let us assume $x(t) = (E_h, I_h, E_m, I_m, I_e)^T$ and hence the system (1) is expressed as

$$\dot{x(t)} = \mathscr{F} - \mathscr{V} \tag{12}$$

$$\text{where} \quad \mathscr{F}(x) = \begin{pmatrix} \frac{\rho(1-c_1)\alpha_1 I_m S_h}{1+kI_m} \\ 0 \\ \rho(1-c_1)\alpha_2 I_h S_m \\ 0 \\ 0 \end{pmatrix} \quad \text{and} \quad \mathscr{V}(x) = \begin{pmatrix} f_1 E_h \\ -\beta_1 E_h + f_2 I_h \\ f_6 E_m \\ -\beta_2 E_m - \phi I_e + f_5 I_m \\ -\theta\pi I_m + f_7 I_e \end{pmatrix}.$$

The Jacobian matrices of above matrices at Q_0 are as follows.

$$F = \begin{pmatrix} 0 & 0 & 0 & \frac{(1-c_1)\alpha_1\rho\Omega}{\mu} & 0 \\ 0 & 0 & 0 & 0 & 0 \\ 0 & \frac{(1-c_1)\alpha_2\rho\phi\Psi}{f_5 f_7} & 0 & 0 & 0 \\ 0 & 0 & 0 & 0 & 0 \\ 0 & 0 & 0 & 0 & 0 \end{pmatrix} \quad \text{and} \quad V = \begin{pmatrix} f_1 & 0 & 0 & 0 & 0 \\ -\beta_1 & f_2 & 0 & 0 & 0 \\ 0 & 0 & f_6 & 0 & 0 \\ 0 & 0 & -\beta_2 & f_5 & -\phi \\ 0 & 0 & 0 & -\pi\theta & f_7 \end{pmatrix}.$$

The next-generation matrix for system (1)is given by

$$F\ V^{-1} = \begin{pmatrix} 0 & 0 & \frac{(1-c_1)f_7\alpha_1\beta_2\rho\Omega}{f_6\mu(f_5 f_7 - \pi\theta\phi)} & \frac{(1-c_1)f_7\alpha_1\rho\Omega}{\mu(f_5 f_7 - \pi\theta\phi)} & \frac{(1-c_1)\alpha_1\rho\Omega\phi}{\mu(f_5 f_7 - \pi\theta\phi)} \\ 0 & 0 & 0 & 0 & 0 \\ \frac{(1-c_1)\alpha_2\beta_1\rho\phi\Psi}{f_1 f_2 f_5 f_7} & \frac{(1-c_1)\alpha_2\rho\phi\Psi}{f_2 f_5 f_7} & 0 & 0 & 0 \\ 0 & 0 & 0 & 0 & 0 \\ 0 & 0 & 0 & 0 & 0 \end{pmatrix}.$$

$\rho\ (FV^{-1})$, the spectral radius of FV^{-1} is the BRN given by:

$$R_0 = \sqrt{\frac{(1-c_1)^2\rho^2\alpha_1\alpha_2\beta_1\beta_2\Psi\phi\Omega}{f_1 f_2 f_5 f_6 \mu(f_5 f_7 - \phi\pi\theta)}} \tag{13}$$

5. Stability Analysis of the Dengue Reinfection Model

This section performs a stability analysis on the endemic equilibrium (EE) point Q_1 and the disease free equilibrium (DFE) point Q_0 and numerically verified in the numerical section. The Hurwitz-Routh criterion and Lasallae's invariance principle are used in the stabilty analysis.

5.1. Local stability analysis of DFE. This subsection discusses about the local stability analysis of DFE. The Hurwitz-Routh criteria is used to define the conditions for the local asymptotic stability of the system (1) around the point Q_0.

Theorem 3. *If $R_0 < 1$ and some few additional conditions are met, the disease-free equilibrium point Q_0 is locally asymptotically stable in Θ.*

Proof. The Jacobian matrix at Q_0 is $J(Q_0)$ given by:

$$J(Q_0) = \begin{pmatrix} -\mu & 0 & 0 & \delta & 0 & 0 & -\frac{\rho(1-c_1)\alpha_1\Omega}{\mu} & 0 & 0 \\ 0 & -f_1 & 0 & 0 & 0 & 0 & \frac{\rho(1-c_1)\alpha_1\Omega}{\mu} & 0 & 0 \\ 0 & \beta_1 & -f_2 & 0 & 0 & 0 & 0 & 0 & 0 \\ 0 & 0 & f_3 & -f_4 & 0 & 0 & 0 & 0 & 0 \\ 0 & 0 & -\frac{\rho(1-c_1)\alpha_2\phi\Psi}{f_5 f_7} & 0 & -f_5 & 0 & 0 & \phi & 0 \\ 0 & 0 & \frac{\rho(1-c_1)\alpha_2\phi\Psi}{f_5 f_7} & 0 & 0 & -f_6 & 0 & 0 & 0 \\ 0 & 0 & 0 & 0 & 0 & \beta_2 & -f_5 & 0 & \phi \\ 0 & 0 & 0 & 0 & 0 & 0 & -\theta\pi & -f_7 & 0 \\ 0 & 0 & 0 & 0 & 0 & 0 & \theta\pi & 0 & -f_7 \end{pmatrix} \tag{14}$$

The determinantal equation of $J(Q_0)$ is given by

$$|J(Q_0) - \lambda I| = 0 \tag{15}$$

simplifying equation (15), we get $(f_4+\lambda)(f_5+\lambda)(f_7+\lambda)(\lambda+\mu)P(\lambda) = 0$, where

$$P(\lambda) = \lambda^5 + B_1\lambda^4 + B_2\lambda^3 + B_3\lambda^2 + B_4\lambda + B_5 \tag{16}$$

$$\begin{aligned} B_1 &= f_1 + f_2 + f_5 + f_6 + f_7 \\ B_2 &= f_5 f_6 + (f_5 + f_6) f_7 + f_2(f_5 + f_6 + f_7) + f_1(f_2 + f_5 + f_6 + f_7) - \pi\theta\phi \\ B_3 &= f_2 f_5 f_6 + f_2 f_5 f_7 + f_2 f_6 f_7 + f_5 f_6 f_7 - (f_2 + f_6)\pi\theta\phi + f_1(f_5 f_6 + (f_5 + f_6) f_7 \\ &\quad + f_2(f_5 + f_6 + f_7) - \pi\theta\phi) \\ B_4 &= f_2 f_6(f_5 f_7 - \pi\theta\phi) + f_1(f_2 f_5 f_6 + f_2 f_5 f_7 + f_2 f_6 f_7 + f_5 f_6 f_7 - (f_2 + f_6)\pi\theta\phi) \\ &\quad - \frac{((1-c_1)^2\alpha_1\alpha_2\beta_1\beta_2\rho^2\phi\ \Psi\Omega)}{f_5 f_7 \mu} \end{aligned} \tag{17}$$

$$
\begin{aligned}
B_5 &= f_1 f_2 f_6 (f_5 f_7 - \pi\theta\phi) - \frac{((1-c_1)^2 \alpha_1 \alpha_2 \beta_1 \beta_2 \rho^2 \phi \Psi \Omega)}{f_5 \mu} \\
&= f_1 f_2 f_6 (f_5 f_7 - \pi\theta\phi) \left(1 - R_0^2\right)
\end{aligned} \tag{18}
$$

Obviously $B_1 > 0$ and $B_5 > 0$ if and only if $R_0^2 < 1$. The Hurwitz- Routh criteria states that the polynomial $P(\lambda) = 0$ with real coefficients have all roots negative or roots with negative real parts if and only if $B_i > 0, i = 1,2,3,4,5$, $B_1 B_2 B_3 > B_3^2 + B_1^2 B_4$ and $(B_1 B_4 - B_5)(B_1 B_2 B_3 - B_3^2 - B_1^2 B_4) > B_5 (B_1 B_2 - B_3)^2 + B_1 B_5^2$. Therefore, if $R_0 < 1$ and the aforementioned conditions are met, the DFE point Q_0 is locally asymptotically stable; otherwise, it is unstable. □

5.2. Global stability analysis of DFE. Using the conditions of the Castillo-Chavez technique [71], we analyse the global asymptotic stability (GAS) of Q_0 based on the value of R_0 in this section. The feasible region $\Theta_1 = \{(S_h, E_h, I_h, R_h, S_m, E_m, I_m, S_e, I_e) \in \Theta : S_h \leq S_h^0, S_m \leq S_m^0, S_e \leq S_e^0\}$ is used to demonstrate the GAS of Q_0. First, the positively invariant property of the region Θ_1 is established. It is obvious that $\Theta_1 \subseteq \Theta$

Theorem 4. *The region* $\Theta_1 = \{(S_h, E_h, I_h, R_h, S_m, E_m, I_m, S_e, I_e) \in \Theta : S_h \leq S_h^0, S_m \leq S_m^0, S_e \leq S_e^0\}$ *is a positively invariant set for the Dengue system (1)*

Proof. From Dengue system (1), we obtain

$$
\begin{aligned}
\dot{S_h} &= \Omega - \frac{\rho(1-c_1)\alpha_1 I_m S_h}{1 + k I_m} - \mu S_h + \delta R_h \\
&\leq \Omega - \mu S_h + \delta R_h
\end{aligned} \tag{19}
$$

Here $\dot{S_h} \leq \Omega - \mu S_h + \delta R_h$ for all values of $R_h(t) \geq 0$. Hence

$$
\dot{S_h} \leq \Omega - \mu S_h \tag{20}
$$

If $S_h(0) \in \Theta_1$, then $S_h(0) \leq S_h^0$. Hence

$$
S_h(t) \leq -(S_h^0 - S_h(0)) e^{-\mu t} + \frac{\Omega}{\mu} \leq \frac{\Omega}{\mu} = S_h^0 \tag{21}
$$

In Θ_1, $S_e \leq S_e^0$. Hence using $\frac{dS_m}{dt} = \phi S_e - \rho(1-c_1)\alpha_2 I_h S_m - (\xi + pc_3)S_m$, we get,

$$\begin{aligned} \dot{S_m} &= \phi S_e - \rho(1-c_1)\alpha_2 I_h S_m - f_5 S_m \\ &\leq \phi S_e - f_5 S_m \\ &\leq \phi S_e^0 - f_5 S_m \end{aligned} \tag{22}$$

After simplification, we get,

$$\begin{aligned} S_m(t) &\leq -\left(\frac{\phi S_e^0}{f_5} - S_m(0)\right) e^{-f_5 t} + \frac{\phi S_e^0}{f_5} = -\left(S_m^0 - S_m(0)\right) e^{-f_5 t} + S_m^0 \\ &\leq S_m^0 \end{aligned} \tag{23}$$

Hence , $S_h \leq S_h^0$, $S_m \leq S_m^0$ $\forall t \geq 0$ if the preliminary conditions $(S_h(0), S_m(0), S_e(0)) \in \Theta_1$. The region Θ_1 is thus a positively invariant set that draws all of the system (1) solutions in $\mathbb{R}_+^9$. □

Theorem 5. *The DEF point Q_0 in Θ_1 is GAS If $R_0 < 1$.*

Proof. The system (1) is expressed by

$$\dot{X} = K(X,I),\ \dot{I} \ = L(X,I) \tag{24}$$

Where, in this instance, dot indicates differentiation with respect to t, $X = (S_h, S_m, S_e, R_h)^T$, $I = (E_h, E_m, I_h, I_m, I_e)^T$,

$$K(X,I) = \begin{pmatrix} \Omega - \frac{\rho(1-c_1)\alpha_1 I_m S_h}{1+kI_m} - \mu S_h + \delta R_h \\ \phi S_e - \rho(1-c_1)\alpha_2 I_h S_m - f_5 S_m \\ \Psi - \theta\pi I_m - f_7 S_e \\ f_3 I_h - f_4 R_h \end{pmatrix}, L(X,I) = \begin{pmatrix} \frac{\rho(1-c_1)\alpha_1 I_m S_h}{1+kI_m} - f_1 E_h \\ \rho(1-c_1)\alpha_2 I_h S_m - f_6 E_m \\ \beta_1 E_h - f_2 I_h \\ \beta_2 E_m + \phi I_e - f_5 I_m \\ \theta\pi I_m - f_7 I_e \end{pmatrix}$$

Further more

$$D = \begin{pmatrix} -f_1 & 0 & 0 & \frac{\rho(1-c_1)\alpha_1\Omega}{\mu} & 0 \\ 0 & -f_6 & \frac{\rho(1-c_1)\alpha_2\phi\Psi}{f_5 f_7} & 0 & 0 \\ \beta_1 & 0 & -f_2 & 0 & 0 \\ 0 & \beta_2 & 0 & -f_5 & \phi \\ 0 & 0 & 0 & \theta\pi & -f_7 \end{pmatrix},\ \hat{L}(X,I) = \begin{pmatrix} \rho(1-c_1)\alpha_1 \left(S_h^0 - \frac{S_h}{1+kI_m}\right) I_m \\ \rho(1-c_1)\alpha_2 \left(S_m^0 - S_m\right) I_h \\ 0 \\ 0 \\ 0 \end{pmatrix}$$

$$K(X,I)\Big|_{I=0} = \begin{pmatrix} \Omega - \mu S_h + \delta R_h \\ \phi S_e - f_5 S_m \\ \Psi - f_7 S_e \\ -f_4 R_h \end{pmatrix}, L(X,I)\Big|_{I=0} = \begin{pmatrix} 0 \\ 0 \\ 0 \\ 0 \\ 0 \end{pmatrix}, \text{ where } D = L_I(X^*,0),\ \ L(X,I) = DI - \hat{L}(X,I)$$

Solving the system $\frac{dX}{dt} = K(X,0)$, we get $\frac{dR_h}{dt} = -f_4 R_h$, $\frac{dS_h}{dt} = \Omega - \mu S_h + \delta R_h$, $\frac{dS_m}{dt} = \phi S_e - f_5 S_m$ and $\frac{dS_e}{dt} = \Psi - f_7 S_e$ and after simplifying, we get $\lim_{t\to\infty} R_h(t) = 0$, $\lim_{t\to\infty} S_e(t) = S_e^0$, and $\lim_{t\to\infty} S_h(t) = S_h^0$ respectively. The solutions of $\frac{dX}{dt} = K(X,0)$ does not always depend on the initial conditions $S_h(0)$, $S_m(0)$, $S_e(0)$ and $R_h(0)$. As a result, for the solution ($S_h(t)$, $S_m(t)$, $S_e(t)$ $R_h(t)$) of $\frac{dX}{dt} = K(X,0)$, the asymptotic nature is independent of the conditions (2) in Θ_1, assuring that the equilibrium point $X^* = (S_h^0, S_m^0, S_e^0, R_h^0)$ is globally asymptotically stable and as a result, the first condition of the Castillo-Chavez approach [71] is met. Further in Θ_1, $S_h \le S_h^0, S_m \le S_m^0, S_e \le S_e^0$ and hence in the region Θ_1,

$$\rho(1-c_1)\alpha_1 \left(S_h^0 - \frac{S_h}{1+kI_m} \right) I_m \ge \rho(1-c_1)\alpha_1 \left(S_h^0 - S_h \right) I_m \ge 0 \tag{25}$$

$$\rho(1-c_1)\alpha_2 \left(S_m^0 - S_m \right) I_h \ge 0 \tag{26}$$

Hence $\hat{L}(X,I) \ge 0$, which satisfies the condition-2 of Castillo-Chavez method [71]. As a result, Q_0 is GAS in Θ_1 if $R_0 < 1$. □

5.3. Endemic equilibrium. In this section, we examine the local asymptotic stability (LAS) and global asymptotic stability (GAS) of Q_1.

5.3.1. *Local asymptotic stability of endemic equilibrium.*

Theorem 6. *If $R_0 > 1$ and all of the conditions in the proof are satisfied, the EE point Q_1 of the system (1) is LAS in $\Upsilon \subseteq \Theta$.*

Proof.

(27)

$$J(Q_1)=\begin{pmatrix}
-\frac{\rho(1-c_1)\alpha_1 I_m^*}{1+kI_m^*}-\mu & 0 & 0 & \delta & 0 & 0 & -\frac{\rho(1-c_1)\alpha_1 S_h^*}{(1+kI_m^*)^2} & 0 & 0\\
\frac{\rho(1-c_1)\alpha_1 I_m^*}{1+kI_m^*} & -f_1 & 0 & 0 & 0 & 0 & \frac{\rho(1-c_1)\alpha_1 S_h^*}{(1+kI_m^*)^2} & 0 & 0\\
0 & \beta_1 & -f_2 & 0 & 0 & 0 & 0 & 0 & 0\\
0 & 0 & f_3 & -f_4 & 0 & 0 & 0 & 0 & 0\\
0 & 0 & -\rho(1-c_1)\alpha_2 S_m^* & 0 & -(\rho(1-c_1)\alpha_2 I_h^*+f_5) & 0 & 0 & \phi & 0\\
0 & 0 & \rho(1-c_1)\alpha_2 S_m^* & 0 & \rho(1-c_1)\alpha_2 I_h^* & -f_6 & 0 & 0 & 0\\
0 & 0 & 0 & 0 & 0 & \beta_2 & -f_5 & 0 & \phi\\
0 & 0 & 0 & 0 & 0 & 0 & -\theta\pi & -f_7 & 0\\
0 & 0 & 0 & 0 & 0 & 0 & \theta\pi & 0 & -f_7
\end{pmatrix}$$

The characteristic polynomial of (27) is given by

$$|J(Q_1)-\lambda I|=0 \tag{28}$$

The polynomial in λ is

$$(\lambda+f_7)P(\lambda)=0 \tag{29}$$

where

$$P(\lambda)=\lambda^8+b_1\lambda^7+b_2\lambda^6+b_3\lambda^5+b_4\lambda^4+b_5\lambda^3+b_6\lambda^2+b_7\lambda+b_8 \tag{30}$$

One latent roots of (29) is $\lambda=-f_7<0$. The remaining latent roots of (29) are analysed using the polynomial equation $P(\lambda)$

The coefficients of (30) are as follows:

$$b_1=-a_1-a_4+f_1+f_2+f_4+f_5+f_6+f_7 \tag{31}$$

$$\begin{aligned} b_2=\ & f_1f_2+f_1f_4+f_2f_4+f_1f_5+f_2f_5+f_4f_5+f_1f_6+f_2f_6+f_4f_6+f_5f_6+a_1(a_4-f_1-f_2-f_4\\ & -f_5-f_6-f_7)+(f_1+f_2+f_4+f_5+f_6)f_7-a_4(f_1+f_2+f_4+f_5+f_6+f_7)-\pi\theta\phi \end{aligned} \tag{32}$$

$$\begin{aligned} b_3=\ & f_1f_2f_4+f_1f_2f_5+f_1f_4f_5+f_2f_4f_5+f_1f_2f_6+f_1f_4f_6+f_2f_4f_6+f_1f_5f_6+f_2f_5f_6+\\ & f_4f_5f_6+f_1f_2f_7+f_1f_4f_7+f_2f_4f_7+f_1f_5f_7+f_2f_5f_7+f_4f_5f_7+f_1f_6f_7+f_2f_6f_7+\\ & f_4f_6f_7+f_5f_6f_7-f_1\pi\theta\phi-f_2\pi\theta\phi-f_4\pi\theta\phi-f_6\pi\theta\phi-a_4(f_4f_5+f_4f_6+f_5f_6+(f_4+\\ & f_5+f_6)f_7+f_2(f_4+f_5+f_6+f_7)+f_1(f_2+f_4+f_5+f_6+f_7)-\pi\theta\phi)-a_1(f_2f_4+\\ & f_2f_5+f_4f_5+f_2f_6+f_4f_6+f_5f_6+(f_2+f_4+f_5+f_6)f_7+f_1(f_2+f_4+f_5+f_6+f_7)-\\ & a_4(f_1+f_2+f_4+f_5+f_6+f_7)-\pi\theta\phi) \end{aligned} \tag{33}$$

(34)

$$b_4 = f_1f_2f_4f_5 + f_1f_2f_4f_6 + f_1f_2f_5f_6 + f_1f_4f_5f_6 + f_2f_4f_5f_6 - a_4(f_2f_4f_5 + f_4f_5f_6 + f_2(f_4 + f_5)f_6 + f_1(f_4f_5 + (f_4 + f_5)f_6 + f_2(f_4 + f_5 + f_6))) + f_1f_2f_4f_7 + f_1f_2f_5f_7 + f_1f_4f_5f_7 + f_2f_4f_5f_7 + f_1f_2f_6f_7 + f_1f_4f_6f_7 + f_2f_4f_6f_7 + f_1f_5f_6f_7 + f_2f_5f_6f_7 + f_4f_5f_6f_7 - a_4(f_4f_5 + (f_4 + f_5)f_6 + f_2(f_4 + f_5 + f_6) + f_1(f_2 + f_4 + f_5 + f_6))f_7 - a_2a_3\beta_1\beta_2 + f_3\beta_1\delta\mu + a_4\pi(f_1 + f_2 + f_4 + f_6 - \beta_2)\theta\phi - \pi(f_4f_6 + f_2(f_4 + f_6) + f_1(f_2 + f_4 + f_6) + f_5\beta_2)\theta\phi + a_1(-f_2f_4f_5 - f_2f_4f_6 - f_2f_5f_6 - f_4f_5f_6 - f_2f_4f_7 - f_2f_5f_7 - f_4f_5f_7 - f_2f_6f_7 - f_4f_6f_7 - f_5f_6f_7 + f_3\beta_1\delta + (f_2 + f_4 + f_6)\pi\theta\phi - f_1(f_5f_6 + (f_5 + f_6)f_7 + f_4(f_5 + f_6 + f_7) + f_2(f_4 + f_5 + f_6 + f_7) - \pi\theta\phi) + a_4(f_4f_5 + f_4f_6 + f_5f_6 + (f_4 + f_5 + f_6)f_7 + f_2(f_4 + f_5 + f_6 + f_7) + f_1(f_2 + f_4 + f_5 + f_6 + f_7) - \pi\theta\phi))$$

(35)

$$b_5 = f_1f_2f_4f_5f_6 + f_1f_2f_4f_5f_7 + f_1f_2f_4f_6f_7 + f_1f_2f_5f_6f_7 + f_1f_4f_5f_6f_7 + f_2f_4f_5f_6f_7 - a_2a_3f_4\beta_1\beta_2 - a_2a_3f_5\beta_1\beta_2 - a_2a_3f_7\beta_1\beta_2 - a_2a_3\beta_1\beta_2\mu + f_3f_5\beta_1\delta\mu + f_3f_6\beta_1\delta\mu + f_3f_7\beta_1\delta\mu - a_4(f_2f_4f_5f_6 + (f_2f_4f_5 + f_4f_5f_6 + f_2(f_4 + f_5)f_6)f_7 + f_1(f_4f_5f_6 + f_5f_6f_7 + f_4(f_5 + f_6)f_7 + f_2(f_5f_6 + (f_5 + f_6)f_7 + f_4(f_5 + f_6 + f_7))) + f_3\beta_1\delta\mu) + a_4\pi(f_2f_4 + f_2f_6 + f_4f_6 + f_1(f_2 + f_4 + f_6 - \beta_2) - (f_2 + f_4)\beta_2)\theta\phi - \pi(f_1f_2f_4 + f_1f_2f_6 + f_1f_4f_6 + f_2f_4f_6 + (f_1 + f_2 + f_4)f_5\beta_2)\theta\phi + a_1(-f_2f_4f_5f_6 - f_2f_4f_5f_7 - f_2f_4f_6f_7 - f_2f_5f_6f_7 - f_4f_5f_6f_7 - f_1(f_4f_5f_6 + f_5f_6f_7 + f_4(f_5 + f_6)f_7 + f_2(f_5f_6 + (f_5 + f_6)f_7 + f_4(f_5 + f_6 + f_7))) + f_3f_5\beta_1\delta + f_3f_6\beta_1\delta + f_3f_7\beta_1\delta + f_1(f_2 + f_4 + f_6)\pi\theta\phi + \pi(f_4f_6 + f_2(f_4 + f_6) + f_5\beta_2)\theta\phi + a_4(f_4f_5f_6 + f_4f_5f_7 + f_4f_6f_7 + f_5f_6f_7 - f_3\beta_1\delta - \pi(f_4 + f_6 - \beta_2)\theta\phi + f_2(f_6f_7 + f_5(f_6 + f_7) + f_4(f_5 + f_6 + f_7) - \pi\theta\phi) + f_1(f_5f_6 + (f_5 + f_6)f_7 + f_4(f_5 + f_6 + f_7) + f_2(f_4 + f_5 + f_6 + f_7) - \pi\theta\phi)))$$

(36)

$$b_6 = f_1f_2f_4f_5f_6f_7 - a_4(f_1f_2f_4f_5f_6 + f_2f_4f_5f_6f_7 + f_1(f_2f_4f_5 + f_4f_5f_6 + f_2(f_4 + f_5)f_6)f_7) - a_2a_3f_4f_5\beta_1\beta_2 - a_2a_3f_4f_7\beta_1\beta_2 - a_2a_3f_5f_7\beta_1\beta_2 - a_2a_3f_4\beta_1\beta_2\mu - a_2a_3f_5\beta_1\beta_2\mu - a_2a_3f_7\beta_1\beta_2\mu + f_3f_5f_6\beta_1\delta\mu + f_3f_5f_7\beta_1\delta\mu + f_3f_6f_7\beta_1\delta\mu - a_4f_3(f_5 + f_6 + f_7)\beta_1\delta\mu + a_4\pi(f_2f_4(f_6 - \beta_2) + f_1(f_2f_4 + f_2f_6 + f_4f_6 - (f_2 + f_4)\beta_2))\theta\phi - \pi\theta(f_1f_2f_4f_6 + f_2f_4f_5\beta_2 + f_1(f_2 + f_4)f_5\beta_2 + f_3\beta_1\delta\mu)\phi + a_1(-f_2f_4f_5f_6f_7 - f_1(f_2f_4f_5f_6 + (f_2f_4f_5 + f_4f_5f_6 + f_2(f_4 + f_5)f_6)f_7) + f_3f_5f_6\beta_1\delta + f_3f_5f_7\beta_1\delta + f_3f_6f_7\beta_1\delta + f_1\pi(f_4f_6 + f_2(f_4 + f_6) + f_5\beta_2)\theta\phi + \pi(f_2f_4f_6 + (f_2 + f_4)f_5\beta_2 - f_3\beta_1\delta)\theta\phi + a_4(f_2f_4f_5f_6 + f_2f_4f_5f_7 + f_2f_4f_6f_7 + f_2f_5f_6f_7 + f_4f_5f_6f_7 - f_3f_5\beta_1\delta - f_3f_6\beta_1\delta - f_3f_7\beta_1\delta - \pi(f_2f_4 + f_2f_6 + f_4f_6 - (f_2 + f_4)\beta_2)\theta\phi + f_1(f_4f_5f_6 + f_4f_5f_7 + f_4f_6f_7 + f_5f_6f_7 - \pi(f_4 + f_6 - \beta_2)\theta\phi + f_2(f_5f_6 + (f_5 + f_6)f_7 + f_4(f_5 + f_6 + f_7) - \pi\theta\phi))))$$

(37)

$$b_7 = f_3f_5f_6f_7\beta_1\delta\mu - a_2a_3\beta_1\beta_2(f_4f_5f_7 + f_5f_7\mu + f_4(f_5 + f_7)\mu) - \pi\theta(f_1f_2f_4f_5\beta_2 + f_3f_6\beta_1\delta\mu)\phi + a_4(-f_3\beta_1\delta\mu(f_6f_7 + f_5(f_6 + f_7) - \pi\theta\phi) - f_1f_2f_4(f_5f_6f_7 + \pi(-f_6 + \beta_2)\theta\phi)) + a_1(f_5f_6f_7(-f_1f_2f_4 + f_3\beta_1\delta) + \pi(f_1f_2f_4f_6 + f_2f_4f_5\beta_2 + f_1(f_2 + f_4)f_5\beta_2 - f_3f_6\beta_1\delta)\theta\phi + a_4(-f_3\beta_1\delta(f_6f_7 + f_5(f_6 + f_7) - \pi\theta\phi) + f_2f_4(f_5f_6f_7 + \pi(-f_6 + \beta_2)\theta\phi) + f_1(f_2f_4f_5f_6 + f_2f_4f_5f_7 + f_2f_4f_6f_7 + f_2f_5f_6f_7 + f_4f_5f_6f_7 - \pi(f_2f_4 + f_2f_6 + f_4f_6 - (f_2 + f_4)\beta_2)\theta\phi)))$$

(38)
$$b_8 = a_1(f_1f_2f_4 - f_3\beta_1\delta)(a_4f_5f_6f_7 + \pi(-a_4f_6 + (a_4+f_5)\beta_2)\theta\phi) + \beta_1\mu(-f_5f_7(a_2a_3f_4\beta_2 + a_4f_3f_6\delta) + f_3\pi(a_4f_6 - (a_4+f_5)\beta_2)\delta\theta\phi)$$

Where $a_1 = -\mu - \frac{(1-c_1)I_m^*\alpha_1\rho}{1+I_m^*k}$, $a_2 = -\frac{(1-c_1)S_h^*\alpha_1\rho}{(1+I_m^*k)^2}$, $a_3 = \frac{(1-c_1)I_m^*\alpha_1\rho}{1+I_m^*k}$, $a_4 = -(1-c_1)S_m^*\alpha_2\rho$ and $a_5 = -f_5 - (1-c_1)I_h^*\alpha_2\rho$. In accordance with the Hurwitz-Routh criterion, the polynomial (30) has eight roots that are all either negative or have roots that have negative real parts if and only if the determinants of all Hurwitz matrices $H_j, j = 1,2,3,...,8$ are positive.

The Hurwitz matrices are defined follows:

(39)
$$H_1 = (b_1), H_2 = \begin{bmatrix} b_1 & 1 \\ b_3 & b_2 \end{bmatrix}, H_3 = \begin{bmatrix} b_1 & 1 & 0 \\ b_3 & b_2 & b_1 \\ b_5 & b_4 & b_3 \end{bmatrix} \text{ and } H_n = \begin{bmatrix} b_1 & 1 & 0 & 0 & \dots & 0 \\ b_3 & b_2 & b_1 & 1 & \dots & 0 \\ b_5 & b_4 & b_3 & b_2 & \dots & 0 \\ \vdots & \vdots & \vdots & \vdots & \dots & \vdots \\ 0 & 0 & 0 & 0 & \dots & b_n \end{bmatrix}$$

But the EE point Q_1 exists in Υ if $R_0 > 1$ and hence Q_1 is LAS in Υ if $R_0 > 1$ along with the conditions $\det H_j > 0$, $j = 1,2,3,...,8$ are satisfied.

□

5.3.2. *Global asymptotic stability of endemic equilibrium.* This section analyses the global asymptotic stability (GAS) of the endemic equilibrium (EE) point Q_1.

Theorem 7. *If $R_0 > 1$,the EE point Q_1 is GAS in $\Upsilon \subseteq \Theta$, if $(-1)^n|D_i| > 0$, $i = 1,2,3,...,9$, where the expression for D_i is mentioned in the proof.*

Proof. Let's construct a suitable Lyapunov function. $L(S_h, E_h, I_h, R_h, S_m, E_m, I_m, S_e, I_e)$ as follows:

(40)
$$L = \left(S_h - S_h^* + S_h^*\log\left(\frac{S_h^*}{S_h}\right)\right) + \left(E_h - E_h^* + E_h^*\log\left(\frac{E_h^*}{E_h}\right)\right) + \left(I_h - I_h^* + I_h^*\log\left(\frac{I_h^*}{I_h}\right)\right) + \left(R_h - R_h^* + R_h^*\log\left(\frac{R_h^*}{R_h}\right)\right) + \left(S_m - S_m^* + S_m^*\log\left(\frac{S_m^*}{S_m}\right)\right) + \left(E_m - E_m^* + E_m^*\log\left(\frac{E_m^*}{E_m}\right)\right) + \left(I_m - I_m^* + I_m^*\log\left(\frac{I_m^*}{I_m}\right)\right)$$

Using the EE point Q_1 in $\dot{L}$, we get,

$$\frac{dL}{dt} = \left(\frac{S_h-S_h^*}{S_h}\right)\frac{dS_h}{dt} + \left(\frac{E_h-E_h^*}{E_h}\right)\frac{dE_h}{dt} + \left(\frac{I_h-I_h^*}{I_h}\right)\frac{dI_h}{dt} + \left(\frac{R_h-R_h^*}{R_h}\right)\frac{dR_h}{dt} + \left(\frac{S_m-S_m^*}{S_m}\right)\frac{dS_m}{dt} + \left(\frac{E_m-E_m^*}{E_m}\right)\frac{dE_m}{dt} + \left(\frac{I_m-I_m^*}{I_m}\right)\frac{dI_m}{dt} + \left(\frac{S_e-S_e^*}{S_e}\right)\frac{dS_e}{dt} + \left(\frac{I_e-I_e^*}{I_e}\right)\frac{dI_e}{dt} \tag{41}$$

Using Q_1 in the system (1), we get, $\Omega - \frac{\rho(1-c_1)\alpha_1 I_m^* S_h^*}{1+kI_m^*} - \mu S_h^* + \delta R_h^* = 0$, $\frac{\rho(1-c_1)\alpha_1 I_m^* S_h^*}{1+kI_m^*} - f_1 E_h^* = 0$, $\beta_1 E_h^* - f_2 I_h^* = 0$, $f_3 I_h^* - f_4 R_h^* = 0$, $\phi S_e^* - \rho(1-c_1)\alpha_2 I_h^* S_m^* - f_5 S_m^* = 0$, $\rho(1-c_1)\alpha_2 I_h^* S_m^* - f_6 E_m^* = 0$, $\beta_2 E_m^* + \phi I_e^* - f_5 I_m^* = 0$, $\Psi - \theta\pi I_m^* - f_7 S_e^* = 0$, $\theta\pi I_m^* - f_7 I_e^* = 0$. Hence

$$\left(\frac{S_h-S_h^*}{S_h}\right)\frac{dS_h}{dt} = -\left(\frac{\Omega+\delta R_h^*}{S_h S_h^*}\right)(S_h-S_h^*)^2 - \frac{\rho(1-c_1)\alpha_1}{(1+kI_m)(1+kI_m^*)}(I_m-I_m^*)(S_h-S_h^*) + \frac{\delta}{S_h}(S_h-S_h^*)(R_h-R_h^*)$$

$$\left(\frac{E_h-E_h^*}{E_h}\right)\frac{dE_h}{dt} = \frac{\rho(1-c_1)\alpha_1 I_m}{E_h(1+kI_m)}(S_h-S_h^*)(E_h-E_h^*) + \frac{\rho(1-c_1)\alpha_1 S_h^*}{E_h(1+kI_m)(1+kI_m^*)}(E_h-E_h^*)(I_m-I_m^*)$$

$$\left(\frac{I_h-I_h^*}{I_h}\right)\frac{dI_h}{dt} = -\frac{f_2}{I_h}(I_h-I_h^*)^2 + \frac{\beta_1}{I_h}(E_h-E_h^*)(I_h-I_h^*)$$

$$\left(\frac{R_h-R_h^*}{R_h}\right)\frac{dR_h}{dt} = -\frac{f_4}{R_h}(R_h-R_h^*)^2 + \frac{f_3}{R_h}(I_h-I_h^*)(R_h-R_h^*)$$

$$\left(\frac{S_m-S_m^*}{S_m}\right)\frac{dS_m}{dt} = \frac{\rho(1-c_1)\alpha_2(I_h+f_5)}{S_m}(S_m-S_m^*)^2 + \frac{\phi}{S_m}(S_m-S_m^*)(S_e-S_e^*) - \frac{\rho(1-c_1)\alpha_2}{S_m}(S_m-S_m^*)(I_h-I_h^*)$$

$$\left(\frac{E_m-E_m^*}{E_m}\right)\frac{dE_m}{dt} = -\frac{f_6}{E_m}(E_m-E_m^*)^2 + \frac{\rho(1-c_1)\alpha_2 I_h}{E_m}(S_m-S_m^*)(E_m-E_m^*) + \frac{\rho(1-c_1)\alpha_2 S_m^*}{E_m}(E_m-E_m^*)(I_h-I_h^*)$$

$$\left(\frac{I_m-I_m^*}{I_m}\right)\frac{dI_m}{dt} = -\frac{f_5}{I_m}(I_m-I_m^*)^2 + \frac{\beta_2}{I_m}(E_m-E_m^*)(I_m-I_m^*) + \frac{\phi}{I_m}(I_m-I_m^*)(I_e-I_e^*)$$

$$\left(\frac{S_e-S_e^*}{S_e}\right)\frac{dS_e}{dt} = -\frac{f_7}{S_e}(S_e-S_e^*)^2 - \frac{\theta\pi}{S_e}(I_m-I_m^*)(S_e-S_e^*)$$

$$\left(\frac{I_e-I_e^*}{I_e}\right)\frac{dI_e}{dt} = -\frac{f_7}{I_e}(I_e-I_e^*)^2 + \frac{\theta\pi}{I_e}(I_m-I_m^*)(I_e-I_e^*)$$

Now, we express $\dot{L} = Y^T MY$, where

$Y^T = \left(S_h - S_h^* \quad E_h - E_h^* \quad I_h - I_h^* \quad R_h - R_h^* \quad S_m - S_m^* \quad E_m - E_m^* \quad I_m - I_m^* \quad S_e - S_e^* \quad I_e - I_e^*\right)$ and $M = (m_{ij})$, $1 \leq i, j \leq 9$ is a real and symmetric matrix and $m_{11} = -\left(\frac{\Omega + \delta R_h^*}{S_h S_h^*}\right)$, $m_{22} = 0$, $m_{33} = -\frac{f_2}{I_h}$, $m_{44} = -\frac{f_4}{R_h}$, $m_{55} = \frac{\rho(1-c_1)\alpha_2(I_h+f_5)}{S_m}$, $m_{66} = -\frac{f_6}{E_m}$, $m_{77} = -\frac{f_5}{I_m}$, $m_{88} = -\frac{f_7}{S_e}$, $m_{99} = -\frac{f_7}{I_e}$, $m_{12} = m_{21} = \frac{\rho(1-c_1)\alpha_1 I_m}{2(1+kI_m)E_h}$, $m_{13} = m_{31} = 0$, $m_{14} = m_{41} = \frac{\delta}{2S_h}$, $m_{15} = m_{51} = 0$, $m_{16} = m_{61} = 0, m_{17} = m_{71} = 0, m_{18} = m_{81} = 0, m_{19} = m_{91} = 0, m_{23} = m_{32} = \frac{\beta_1}{2I_h}, m_{24} = m_{42} = 0$, $m_{25} = m_{52} = 0, m_{26} = m_{562} = 0, m_{28} = m_{82} = 0, m_{29} = m_{92} = 0, m_{27} = m_{72} = \frac{\rho(1-c_1)\alpha_1 S_h^*}{2(1+kI_m)(1+kI_m^*)E_h}$, $m_{34} = m_{43} = \frac{f_3}{2R_h}$, $m_{35} = m_{53} = -\frac{\rho(1-c_1)\alpha_2}{2S_m}$, $m_{36} = m_{63} = \frac{\rho(1-c_1)\alpha_2 S_m^*}{2E_m}$, $m_{37} = m_{73} = 0$, $m_{38} = m_{83} = 0$, $m_{39} = m_{93} = 0$, $m_{45} = m_{54} = 0$, $m_{46} = m_{64} = 0$, $m_{47} = m_{74} = 0$, $m_{48} = m_{84} = 0, m_{49} = m_{94} = 0$, $m_{56} = m_{65} = \frac{\rho(1-c_1)\alpha_2 I_h}{2E_m}$, $m_{58} = m_{85} = \frac{\phi}{2S_m}$, $m_{57} = m_{75} = 0$, $m_{59} = m_{95} = 0$, $m_{67} = m_{76} = \frac{\beta_2}{2I-m}$, $m_{68} = m_{86} = 0$, $m_{69} = m_{96} = 0$, $m_{78} = m_{87} = -\frac{\phi\pi}{2S_e}$, $m_{79} = m_{97} = \frac{\phi I_e + \phi\pi I_m}{2I_m I_e}$, $m_{89} = m_{98} = 0$. Here the EE point Q_1 is GAS, if $\dot{L} < 0$ which is same stating that the real quadratic form $Y^T MY$ is negative definite. The real symmetric matrix M must be negative definite for the negativity of the real quadratic form $Y^T MY$ as per the Frobenius theorem . Hence the following condition to be satisfied.

$$\text{If } D_i = \begin{pmatrix} m_{11} & m_{12} & m_{13} & \dots & m_{1i} \\ m_{21} & m_{22} & m_{23} & \dots & m_{2i} \\ \vdots & \dots & \vdots & \dots & \vdots \\ m_{91} & m_{92} & m_{93} & \dots & m_{9i} \end{pmatrix}, \text{ then } (-1)^n |D_i| > 0,\ i = 1, 2, 3, ..., 9.$$

□

6. SENSITIVITY ANALYSIS

Sensitivity analysis was carried out on the system (1) to see how various variables impacted the spread of dengue fever in the host population. In this analysis, the variables that significantly affect the system's Basic Reproduction Number (1) are identified. By analysing the characteristics in connection to the basic reproduction number, the health authorities can more effectively control the spread of the disease. The design of experiments, data assimilation, and the simplification of complicated non-linear models are all aided by sensitivity analysis. The normalised forward sensitivity index of R_0 that depends differentiably

on a parameter m is defined as $\Gamma_m^{R_0} = \frac{\partial R_0}{\partial m}\frac{m}{R_0}$. Here $R_0 = \sqrt{\frac{(1-c_1)^2\rho^2\alpha_1\alpha_2\beta_1\beta_2\Psi\phi\Omega}{f_1f_2f_5f_6\mu(f_5f_7-\phi\pi\theta)}}$, where, $f_1 = \beta_1+\mu, f_2 = \gamma+d+\mu+bc_2, f_3 = \gamma+bc_2, f_4 = \delta+\mu, f_5 = \xi+pc_3, f_6 = \beta_2+\xi+pc_3, f_7 = \phi+pc_3$. The sensitivity index of R_0, which is dependent on a number of characteristics of system (1) , is as follows: $\Gamma_\rho^{R_0} = 1 > 0$, $\Gamma_\Omega^{R_0} = 0.5 > 0$, $\Gamma_\Psi^{R_0} = 0.5 > 0$, $\Gamma_{\alpha_1}^{R_0} = 0.5 > 0$, $\Gamma_{\alpha_2}^{R_0} = 0.5 > 0, \Gamma_{\beta_1}^{R_0} = \frac{0.034}{0.068+\beta_1} > 0, \Gamma_{\beta_2}^{R_0} = \frac{0.036365}{0.07273+\beta_2} > 0, \Gamma_\mu^{R_0} = -\frac{0.00391879+(0.189485+1.5\mu)\mu}{(0.061+\mu)(0.128485+\mu)} < 0$, $\Gamma_\xi^{R_0} = \frac{(\xi(0.0000573353+(-0.0662083-1.5\xi)\xi))}{(0.00273+\xi)(0.06773+\xi)\ (-0.00425168+\xi)}$, $\Gamma_\delta^{R_0} = 0$, $\Gamma_d^{R_0} = -\frac{0.5d}{0.131485+d} < 0$, $\Gamma_k^{R_0} = 0$, $\Gamma_\gamma^{R_0} = -\frac{0.5\gamma}{0.135485+\gamma} < 0$, $\Gamma_b^{R_0} = -\frac{0.5b}{5.54286+b} < 0$, $\Gamma_p^{R_0} = -\frac{p(166.561+p(166.12+(43.4231+2p)p))}{219.758+p(333.123+p(166.12+p(28.9487+p)))} < 0$, $\Gamma_\phi^{R_0} = \frac{0.00151046}{0.00302092+\phi} > 0, \Gamma_\theta^{R_0} = \frac{0.5}{1.07298-\theta} > 0, \Gamma_\pi^{R_0} = \frac{0.5\pi}{0.708374-\pi}, \Gamma_{c_1}^{R_0} = -\frac{c_1}{1-c_1} < 0$, $\Gamma_{c_2}^{R_0} = -\frac{0.0355c_2}{0.194+0.071c_2} < 0, \Gamma_{c_3}^{R_0} = -\frac{c_3(28.8054+c_3(51.565+(24.1929+2c_3)c_3))}{21.1744+c_3(57.6108+c_3(51.565+c_3(16.1286+c_3)))} < 0$. A most sensitive parameter's slight variation will result in a significant quantitative variation. To ensure that a small variation in a least sensitive parameter does not result in a big variation, it is important to accurately estimate it. This way, estimating such least sensitive parameters need not require much effort. Table (4) displays the sensitivity indices of the dengue reinfection model (1) in relation to BRN as well as the baseline value of the parameters considered for sensitivity analysis (R_0). With sensitivity index 1, which shows that an increase (decrease) in the effective mosquito biting rate, ρ by 10% will be immediately followed by an increase (decrease) in R_0 by 10%, it is obvious that mosquito biting is the most sensitive parameter. Similarly, a 10% increase (decrease) in the parameters Ω, Ψ, α_1 and α_2 will be followed immediately by a 5% increase (decrease) in the R_0 value. The parameters p, b, c_1, c_2, and c_3 are significant in the context of epidemiology among those with a negative sensitivity index. The sensitivity index of the parameter p, the effectiveness of the control c_3, is -0.3 for $p = 0.5$. According to figure(5)(B), for instance, an increase in the efficiency of the control c_3, let's say p, by 10% would result in a relative decrease in R_0 value of 3%. Figures (2), (3), (4), (5), (6), (7), (8) shows the sensitivity indices of R_0 relative to various parameters of the system (1).

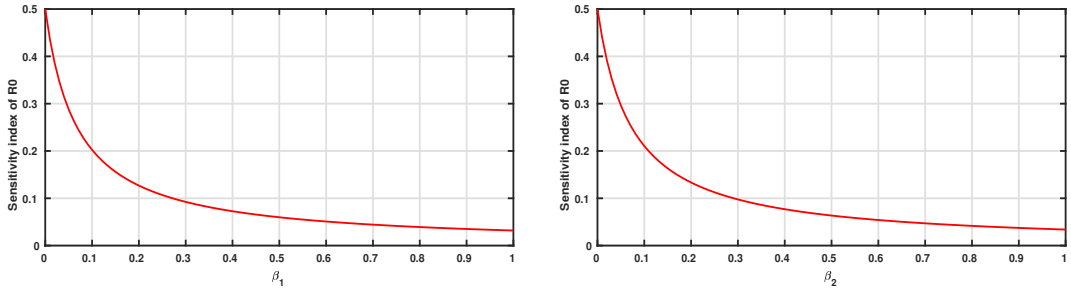

(A) (B)

FIGURE 2. Sensitivity index of R_0 relative to progression rates: (A) Humans exposed to infected, β_1, (B) Vectors exposed to infected, β_2.

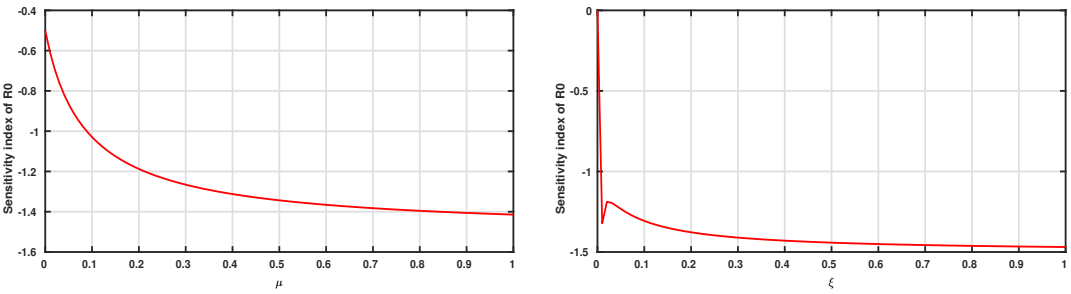

(A) (B)

FIGURE 3. The sensitivity index of R_0 relative to (A) The natural mortality of the human population, μ, (B) The natural death rate of the vector population, ξ.

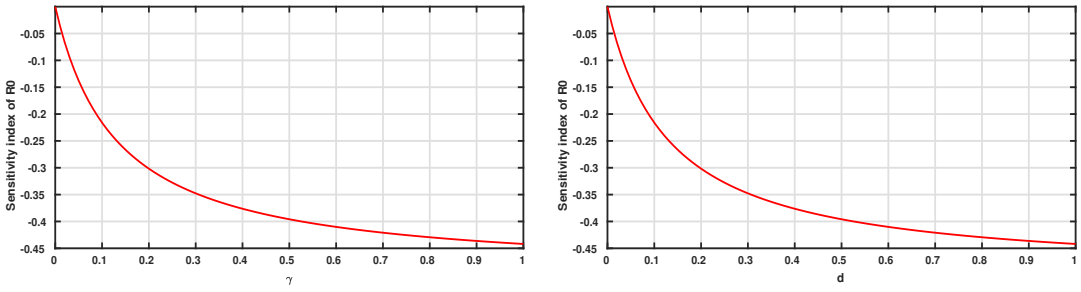

(A) (B)

FIGURE 4. The sensitivity index of R_0 relative to (A) The natural recovery rate of humans from the dengue disease, γ, (B) The disease induced death rate of the humans, d.

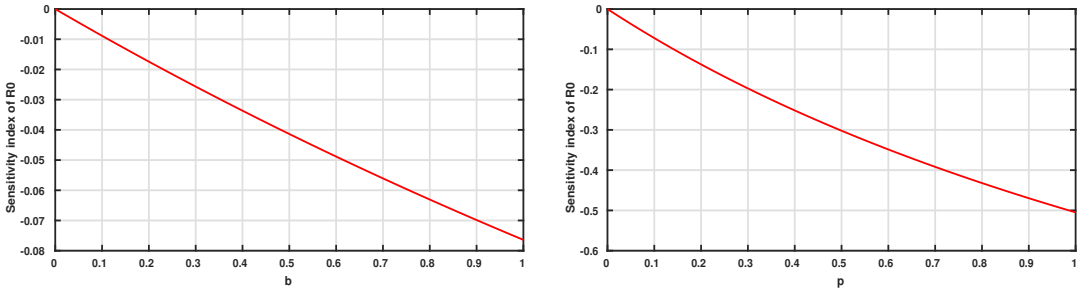

(A) (B)

FIGURE 5. The sensitivity index of R_0 relative to (A) The effectiveness of the control c_2,(B) The effectiveness of the control c_3.

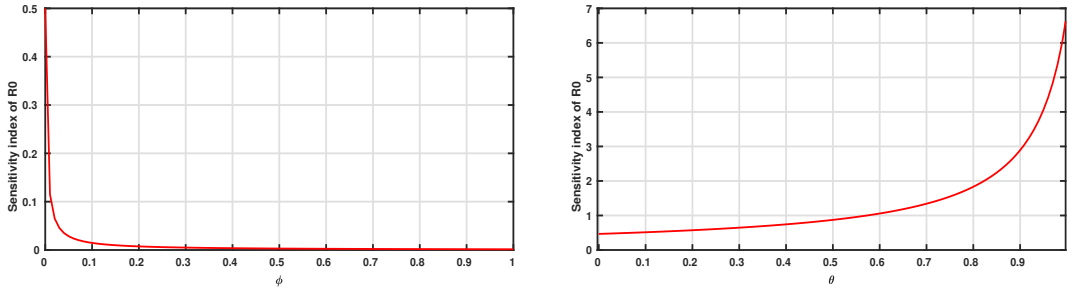

(A) (B)

FIGURE 6. Sensitivity index of R_0 relative to: (A) Development rate of Aedes aeypti mosquitoes, ϕ, (B) Number of Aedes Aegypti mosquito eggs laid per day, θ.

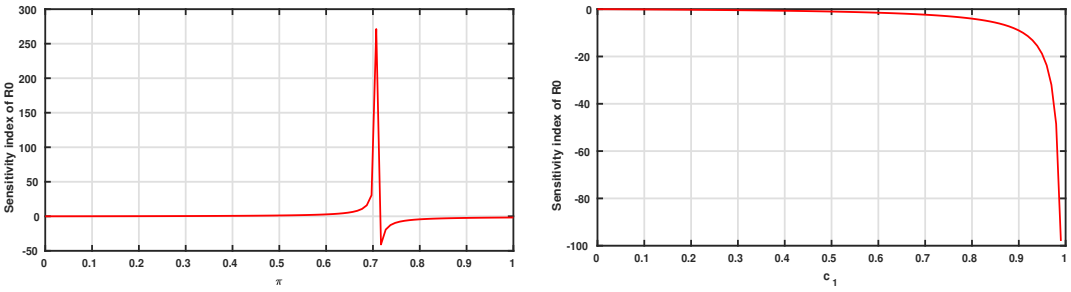

(A) (B)

FIGURE 7. Sensitivity index of R_0 relative to: (A) Vertical transmission rate of Aedes Aeypti mosquitoes, π, (B) Protection control c_1.

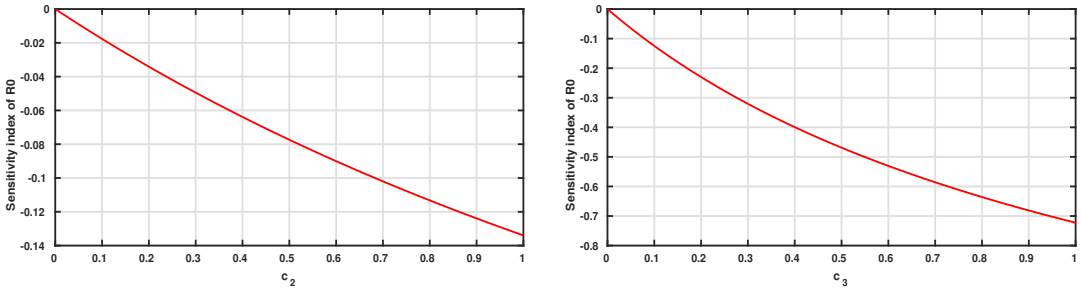

(A) (B)

FIGURE 8. The sensitivity index of R_0 relative to (A) The treatment control c_2 for the humans infected with either of the serotype viruses, (B) The Insecticide spray control c_3 against mosquitoes .

Parameters	**values**	**Sensitivity index**	**Sign of sensitivity index**
ρ	0.331795	$\Gamma_{\rho}^{R_0} = 1$	+
Ω	0.677	$\Gamma_{\Omega}^{R_0} = 0.5$	+
Ψ	0.8	$\Gamma_{\Psi}^{R_0} = 0.5$	+
α_1	0.059	$\Gamma_{\alpha_1}^{R_0} = 0.5$	+
α_2	0.051	$\Gamma_{\alpha_2}^{R_0} = 0.5$	+
β_1	0.061	$\Gamma_{\beta_1}^{R_0} = \frac{0.034}{0.068+\beta_1}$	+
β_2	0.065	$\Gamma_{\beta_2}^{R_0} = \frac{0.036365}{0.07273+\beta_2}$	+
μ	0.068	$\Gamma_{\mu}^{R_0} = -\frac{0.00391879+(0.189485+1.5\mu)\mu}{(0.061+\mu)(0.128485+\mu)}$	-
ξ	0.07	$\Gamma_{\xi}^{R_0} = \frac{(\xi(0.0000573353+(-0.0662083-1.5\xi)\xi))}{(0.00273+\xi)(0.06773+\xi)(-0.00425168+\xi)}$	-
γ	0.061	$\Gamma_{\gamma}^{R_0} = -\frac{0.5\gamma}{0.135485+\gamma}$	-
d	0.065	$\Gamma_{d}^{R_0} = -\frac{0.5d}{0.131485+d}$	-
δ	0.08	$\Gamma_{\delta}^{R_0} = 0$	neutral
k	1	$\Gamma_{k}^{R_0} = 0$	neutral
b	0.071	$\Gamma_{b}^{R_0} = -\frac{0.5b}{5.54286+b}$	-
p	0.07	$\Gamma_{p}^{R_0} = -\frac{p(166.561+p(166.12+(43.4231+2p)p))}{219.758+p(333.123+p(166.12+p(28.9487+p)))}$	-
ϕ	0.854	$\Gamma_{\phi}^{R_0} = \frac{0.00151046}{0.00302092+\phi}$	+
θ	0.103	$\Gamma_{\theta}^{R_0} = \frac{0.5}{1.07298-\theta}$	+
π	0.068	$\Gamma_{\pi}^{R_0} = \frac{0.5\pi}{0.708374-\pi}$	+ / -
c_1	0.025	$\Gamma_{c_1}^{R_0} = -\frac{c_1}{1-c_1}$	-
c_2	0.035	$\Gamma_{c_2}^{R_0} = -\frac{0.0355c_2}{0.194+0.071c_2}$	-
c_3	0.039	$\Gamma_{c_3}^{R_0} = -\frac{c_3(28.8054+c_3(51.565+(24.1929+2c_3)c_3))}{21.1744+c_3(57.6108+c_3(51.565+c_3(16.1286+c_3)))}$	-

TABLE 4. The sensitivity indices of R_0 relative to various parameters of the system (1) with assumed parameter values as given in the table

7. Analysis of Bifurcation in Dengue Reinfection Model

To analyse the bifurcation character of system (1), the Castilla-Chavez and Song [72] technique is applied.

Theorem 8. *When $a < 0$, the system (1) experiences forward bifurcation at $\alpha_1 = \alpha_1^*$ (i.e. at $R_0 = 1$), and the proof provides the expressions for α_1^* and a.*

Proof. Let $S_h = x_1$, $E_h = x_2$, $I_h = x_3$, $R_h = x_4$, $S_m = x_5$, $E_m = x_6$, $I_m = x_7$, $S_e = x_8$, and $I_e = x_9$ and the transformed system is

$$
\begin{aligned}
\dot{x_1} &= \Omega - \frac{\rho(1-c_1)\alpha_1 x_7 x_1}{1+kx_7} - \mu x_1 + \delta x_4 \\
\dot{x_2} &= \frac{\rho(1-c_1)\alpha_1 x_7 x_1}{1+kx_7} - (\beta_1+\mu)x_2 \\
\dot{x_3} &= \beta_1 x_2 - (\gamma+d+\mu+bc_2)x_3 \\
\dot{x_4} &= (\gamma+bc_2)x_3 - (\delta+\mu)x_4 \\
\dot{x_5} &= \phi x_8 - \rho(1-c_1)\alpha_2 x_3 x_5 - (\xi+pc_3)x_5 \\
\dot{x_6} &= \rho(1-c_1)\alpha_2 x_3 x_5 - (\beta_2+\xi+pc_3)x_6 \\
\dot{x_7} &= \beta_2 x_6 + \phi x_9 - (\xi+pc_3)x_7 \\
\dot{x_8} &= \Psi - \theta\pi x_7 - (\phi+pc_3)x_8 \\
\dot{x_9} &= \theta\pi x_7 - (\phi+pc_3)x_9
\end{aligned}
\tag{42}
$$

Human disease transmission rate (α_1) is taken into account as a bifurcation parameter with the constraint $R_0 = 1$. Hence

$$
\alpha_1^* = \frac{\mu(\beta_1+\mu)(bc_2+d+\gamma+\mu)(c_3p+\xi)(c_3p+\beta_2+\xi)(c_3^2p^2+c_3p\xi+c_3p\phi-\pi\theta\phi+\xi\phi)}{(1-2c_1+c_1^2)\alpha_2\beta_1\beta_2\rho^2\phi\psi\Omega}
\tag{43}
$$

DFE of the transformed system (42) is $Q_0 = (x_1^0, x_2^0, x_3^0, x_4^0, x_5^0, x_6^0, x_7^0, x_8^0, x_9^0)$, where $x_1^0 = \frac{\Omega}{\mu} > 0$, $x_2^0 = 0$, $x_3^0 = 0$, $x_4^0 = 0$, $x_5^0 = \frac{\phi\Psi}{f_5 f_7} > 0$, $x_6^0 = 0$, $x_7^0 = 0$, $x_8^0 = \frac{\Psi}{f_7} > 0$, and $x_9^0 = 0$. The linearization matrix of the transformed system (42) at Q_0 is denoted as $J(Q_0)$ at equation (14). One zero eigenvalue exists in the system's jacobian at $\alpha_1 = \alpha_1^*(R_0 = 1)$, but all other eigenvalues have

a negative real part. As a result, using the central manifold theory, the dynamics of the transformed system (42) near to $\alpha_1 = \alpha_1^*(R_0 = 1)$ are studied. According to the central manifold hypothesis [72], the following calculations are necessary.

The right eigenvector for $J(Q_0)$ when $R_0 = 1$ is $W = (w_1, w_2, w_3, w_4, w_5, w_6, w_7, w_8, w_9)^T$ computed using $J(Q_0) \cdot W = 0$ and hence

$w_1 = \frac{\rho\Omega(-1+c_1)w_7\alpha_1(f_1f_2f_4-\delta f_3\beta_1)}{\mu^2 f_1 f_2 f_4}, w_2 = \frac{\rho\Omega(1-c_1)w_7\alpha_1}{\mu f_1}, w_3 = \frac{\rho\Omega(1-c_1)w_7\alpha_1\beta_1}{\mu f_1 f_2},$

$w_4 = \frac{\rho\Omega(1-c_1)f_3w_7\alpha_1\beta_1}{\mu f_1 f_2 f_4},$

$w_8 = -\frac{\pi\theta w_7}{f_7}, w_9 = \frac{\pi\theta w_7}{f_7}, w_5 = -\frac{\phi w_7(\pi\theta\mu f_1 f_2 f_5+\rho^2\psi\Omega\alpha_1\alpha_2\beta_1-2\rho^2\psi\Omega c_1\alpha_1\alpha_2\beta_1+\rho^2\psi\Omega c_1^2\alpha_1\alpha_2\beta_1)}{\mu f_1 f_2 f_5^2 f_7},$

$w_6 = \frac{-\pi\theta\phi w_7+f_5f_7w_7}{f_7\beta_2}$

The left eigenvector of jacobian matrix $J(Q_0)$ when $R_0 = 1$ is V=$(v_1, v_2, v_3, v_4, v_5, v_6, v_7, v_8, v_9)$ computed using $V.J(Q_0) = 0$ and hence we get, $v_i = 0$ for $i = 1,4,5,8$, $v_2 = \frac{\mu(\pi\theta\phi v_7-f_5f_7v_7)}{\rho\Omega(-1+c_1)f_7\alpha_1}$, $v_3 = \frac{(\mu f_1(\pi\theta\phi v_7-f_5f_7v_7)}{\rho\Omega(-1+c_1)f_7\alpha_1\beta_1}$, $v_6 = \frac{v_7\beta_2}{f_6}$, $v_9 = \frac{\phi v_7}{f_7}$. Then, v_7 is computed using the condition $V.W = 1$ and hence

(44)

$$v_7 = \frac{f_1f_2f_6f_7^2}{\pi\theta\phi f_1f_2f_6w_7-\pi\theta\phi f_1f_2f_7w_7-\pi\theta\phi f_1f_6f_7w_7-\pi\theta\phi f_2f_6f_7w_7+f_1f_2f_5f_7^2w_7+f_1f_2f_6f_7^2w_7+f_1f_5f_6f_7^2w_7+f_2f_5f_6f_7^2w_7}$$

The bifurcation coefficients are given by

(45)

$$a = \sum_{k,i,j=1}^{9} v_k w_i w_j \frac{\partial^2 F_k(Q_0, \alpha_1^*)}{\partial x_i \partial x_j}$$

$$b = \sum_{k,i,j=1}^{9} v_k w_i \frac{\partial^2 F_k(Q_0, \alpha_1^*)}{\partial x_i \partial \alpha_1}$$

The following expressions give the bifurcation coefficients a and b after simplification, we get $a = \frac{A_1}{A_2}, b = \frac{B_1}{B_2}$ where $A_1 = 2f_7w_7(\mu f_1f_2f_5^2f_6(-\pi\theta\phi + f_5f_7)(2\mu f_1f_2f_4 + \rho(-1+c_1)\alpha_1(-f_1f_2f_4+\delta f_3\beta_1)) + \rho^2\phi\Omega(-1+c_1)^2f_4\alpha_1\alpha_2\beta_1](\pi\theta\mu f_1f_2f_5 + \rho^2\psi\Omega(-1+c_1)^2\alpha_1\alpha_2\beta_1)\beta_2, A_2 = \mu^2 f_1f_2f_4\, f_5^2((f_2f_5f_6+f_1(f_2f_5+(f_2+f_5)f_6))f_7^2 + \pi\theta\Phi(f_1f_2f_6-(f_2f_6+f_1(f_2+f_6))f_7))$, $B_1 = f_1f_2f_6f_7\ (f_5f_7-\pi\theta\phi)$, $B_2 = ((f_2f_5f_6+f_1(f_2f_5+(f_2+f_5)f_6))f_7^2 + \pi\theta\phi(f_1f_2f_6-(f_2f_6+f_1(f_2+f_6))f_7))\alpha_1$ As a result, when $a < 0$, the system (42) at $R_0 = 1$ experiences forward bifurcation. In forward bifurcation, when $R_0 > 1$, a stable endemic equilibrium coexists with an unstable disease-free equilibrium point. Using the parameter values from table (5), we get $R_0 = 8.94728$, $\alpha_1^* = 0.000206111$, $a = -0.0169782w_7$, $b = 20.437$, $W = (w_1, w_2, w_3, w_4, w_5, w_6, w_7, w_8, w_9)^T$, $V = (v_1, v_2v_3, v_4, v_5, v_6, v_7, v_8, v_9)$, where

$w_1 = -0.0497201w_7,\ w_2 = 0.0219654w_7,\ w_3 = 0.00593772w_7,\ w_4 = 0.00316881w_7,\ w_5 = -1.03352w_7, w_6 = 0.0335247w_7, w_8 = -0.282452w_7, w_9 = 0.282452w_7, v_1 = 0, v_2 = \frac{0.883732}{w_7}, v_3 = \frac{1.2534}{w_7},\ v_4 = 0,\ v_5 = 0,\ v_6 = \frac{0.421353}{w_7},\ v_7 = \frac{0.7615}{w_7},\ v_8 = 0,\ v_9 = \frac{0.699305}{w_7}$. Here $a = -0.0169782w_7 < 0$ and $b = 20.437 > 0$. Hence there exists a forward bifurcation at $\alpha_1 = \alpha_1^* = 0.000206111$ which is represented in figure (9)(A)- (9)(C) relative to the infected compartments of the system (1). The significance of the forward bifurcation at $R_0 = 1$ is that, even though EE and DFE coexist when $R_0 > 1$, the DFE is unstable and the EE is stable, indicating that the disease will likely remain within the host population in the long term. □

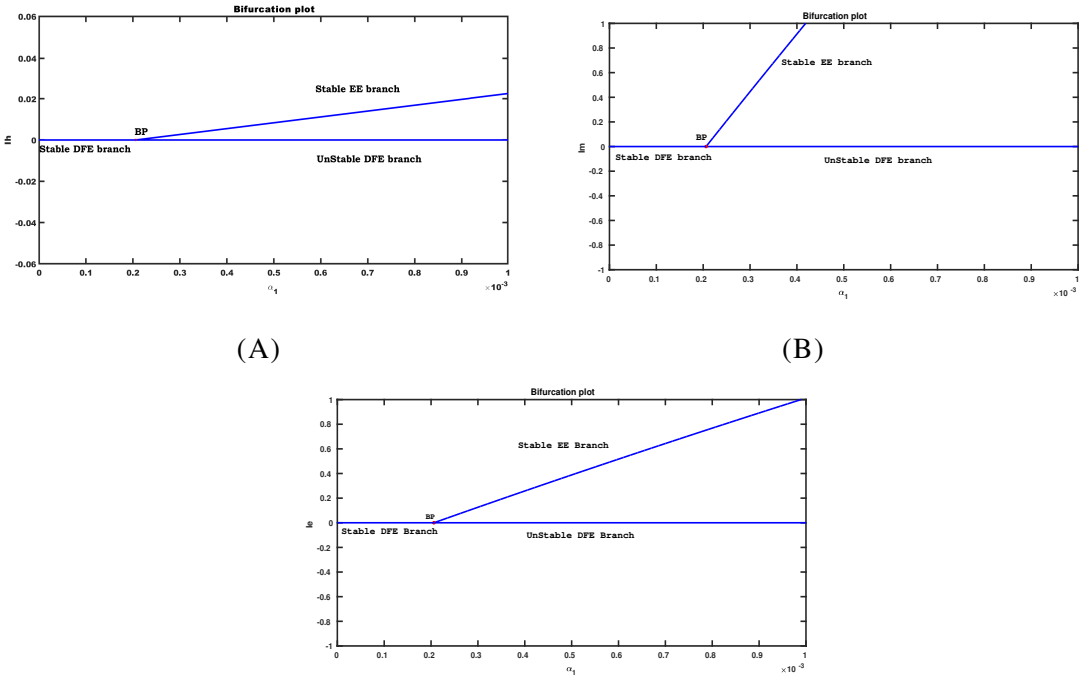

(A) (B)

(C)

FIGURE 9. Bifurcation plot of the infected populations (A) I_h , (B) I_m, (C) I_e against the bifurcation parameter α_1 using the values from table (5)

8. CONTROL PROBLEM WITH OPTIMAL SOLUTIONS

This section examines a system (1) related optimal control problem with three controls. The three control variables used in this optimal control problem are $c_1(t)$, $c_2(t)$, and $c_3(t)$, where $c_1(t)$ denotes a protection control, such as the usage of bed nets or creams to ward off mosquitoes, and $c_2(t)$ indicates treatment control for people who have either of the serotype

viruses, whereas $c_3(t)$ stands for the insecticide spray control that eliminates mosquitoes. Reducing the number of infected individuals, infected vectors, and infected eggs, and the cost of implementing the control strategies are the key goals of this control problem. The control problem with three controls is listed below.

$$
\begin{cases}
\frac{dS_h}{dt} &= \Omega - \frac{\rho(1-c_1(t))\alpha_1 I_m S_h}{1+kI_m} - \mu S_h + \delta R_h \\
\frac{dE_h}{dt} &= \frac{\rho(1-c_1(t))\alpha_1 I_m S_h}{1+kI_m} - (\beta_1 + \mu) E_h \\
\frac{dI_h}{dt} &= \beta_1 E_h - (\gamma + d + \mu + bc_2(t)) I_h \\
\frac{dR_h}{dt} &= (\gamma + bc_2(t)) I_h - (\delta + \mu) R_h \\
\frac{dS_m}{dt} &= \phi S_e - \rho(1-c_1(t))\alpha_2 I_h S_m - (\xi + pc_3(t)) S_m \\
\frac{dE_m}{dt} &= \rho(1-c_1(t))\alpha_2 I_h S_m - (\beta_2 + \xi + pc_3(t)) E_m \\
\frac{dI_m}{dt} &= \beta_2 E_m + \phi I_e - (\xi + pc_3(t)) I_m \\
\frac{dS_e}{dt} &= \Psi - \theta\pi I_m - (\phi + pc_3(t)) S_e \\
\frac{dI_e}{dt} &= \theta\pi I_m - (\phi + pc_3(t)) I_e
\end{cases}
\tag{46}
$$

with preliminary condition(2) and the objective functional [73, 74] is defined as

(47)

$$
\begin{aligned}
J(c_1(t), c_2(t), c_3(t)) = \int_0^{t_e} \big[& W_1 E_h(t) + W_2 I_h(t) + W_3 E_m(t) + W_4 I_m(t) + W_5 I_e(t) + \frac{W_6}{2} c_1^2(t) \\
& + \frac{W_7}{2} c_2^2(t) + \frac{W_8}{2} c_3^2(t) \big] dt
\end{aligned}
$$

Here, W_1, W_2, W_3, W_4 and W_5 represent the corresponding per capita losses caused by the presence of the exposed human population, infected human population, exposed mosquito population, infected mosquito population, and infected egg populations respectively. The constants W_6, W_7 and W_8, respectively, represent the costs involved in the effort to implement protection controls, such as the use of bed nets, mosquito repellent creams, and other similar measures, treatment controls for people infected with either of the serotype viruses and insecticide spray controls that kill mosquitoes. The time interval is assumed to be $[0, t_e]$. The problem is to find the optimal control functions $c_1^*(t)$, $c_2^*(t)$ and $c_3^*(t)$ such that the objective functional $J(c_1(t), c_2(t), c_3(t))$ is minimized, i.e., $J(c_1^*(t), c_2^*(t), c_3^*(t)) = \min\{J(c_1, c_2, c_3); (c_1, c_2, c_3) \in$

$U_c\}$, where the control set U_c is defined as

$U_c = \{(c_1, c_2, c_3); 0 \leq c_i \leq 1, i = 1,2,3;\ c_i$ is Lebesgue measurable function on $[0,1];\ t \in [0, t_e]\}$.

8.1. Existence of the optimal controls. This subsection demonstrates the existence of an optimum control $(c_1^*(t), c_2^*(t), c_3^*(t))$ that minimises the objective functional J subject to the new system (46) with initial conditions (2)).

Theorem 9. *The optimal control $(c_1^*(t), c_2^*(t), c_3^*(t))$ exists for the control system (46) with initial conditions (2) such that $J(c_1^*(t), c_2^*(t), c_3^*(t)) = \min\{J(c_1, c_2, c_3); (c_1, c_2, c_3) \in U_c\}$, with the control set $U_c = \{(c_1, c_2, c_3); 0 \leq c_i \leq 1, i = 1,2,3; t \in [0, t_e]\}$ and c_i is Lebesgue measurable function on $[0,1]$.*

Proof. Since the control system (46) has bounded coefficients, the set of control variables and the accompanying state variables are not empty [75]. The control set U_c is thus by definition closed and convex. Since the state solutions are bounded, the right side of the control system (46) is similarly bounded. Hence, the integrand of the objective functional is convex on U_c. Since the state variables are bounded, there exists constants $l_1 > 0$, $l_2 > 0$ and $p > 1$ such that $W_1 E_h(t) + W_2 I_h(t) + W_3 E_m(t) + W_4 I_m(t) + W_5 I_e(t) + \frac{W_6}{2} c_1^2(t) + \frac{W_7}{2} c_2^2(t) + \frac{W_8}{2} c_3^2(t) \geq l_1(|c_1|^2 + |c_2|^2 + |c_3|^2)^{\frac{p}{2}} - l_2$.

Hence by the properties satisfied as above [75], there exist an optimal control $(c_1^*(t), c_2^*(t), c_3^*(t))$ which minimizes the objective functional J. □

8.2. Characterization. The necessary conditions for the optimal control variables $c_1^*(t)$,$c_2^*(t)$, and $c_3^*(t)$ is derived using the Pontryagin's Maximum Principle [30, 25].

Theorem 10. *For the control system (46), there are optimal control variables $(c_1^*(t), c_2^*(t), c_3^*(t))$, and corresponding solutions $(S_h^*, E_h^*, I_h^*, R_h^*, S_m^*, E_m^*, I_m^*, S_e^*, I_e^*)$ whose objective functional J over Uc is minimised. The existence of continuous functions $\lambda_i(t)$ is related to the explicit optimum control variables.*

Proof. The Hamiltonian is defined as

(48)

$$
\begin{aligned}
H = &\left(W_1E_h(t)+W_2I_h(t)+W_3E_m(t)+W_4I_m(t)+W_5I_e(t)+\frac{W_6}{2}c_1^2(t)+\frac{W_7}{2}c_2^2(t)+\frac{W_8}{2}c_3^2(t)\right)\\
&+\lambda_1\left(\Omega-\frac{\rho(1-c_1(t))\alpha_1I_mS_h}{1+kI_m}-\mu S_h+\delta R_h\right)+\lambda_2\left(\frac{\rho(1-c_1(t))\alpha_1I_mS_h}{1+kI_m}-(\beta_1+\mu)E_h\right)\\
&+\lambda_3\left(\beta_1E_h-(\gamma+d+\mu+bc_2(t))I_h\right)\\
&+\lambda_4\left((\gamma+bc_2(t))I_h-(\delta+\mu)R_h\right)+\lambda_5(\phi S_e-\rho(1-c_1(t))\alpha_2I_hS_m-(\xi+pc_3(t))S_m)\\
&+\lambda_6\left(\rho(1-c_1(t))\alpha_2I_hS_m-(\beta_2+\xi+pc_3(t))E_m\right)+\lambda_7\left(\beta_2E_m+\phi I_e-(\xi+pc_3(t))I_m\right)\\
&+\lambda_8\left(\Psi-\theta\pi I_m-(\phi+pc_3(t))S_e\right)+\lambda_9\left(\theta\pi I_m-(\phi+pc_3(t))I_e\right)
\end{aligned}
$$

where the adjoint functions $\lambda_i(t)$, $i=1$ to 9 to be determined.

Using, $\frac{d\lambda_1}{dt}=-\frac{\partial H}{\partial S_h}$, $\frac{d\lambda_2}{dt}=-\frac{\partial H}{\partial E_h}$, $\frac{d\lambda_3}{dt}=-\frac{\partial H}{\partial I_h}$, $\frac{d\lambda_4}{dt}=-\frac{\partial H}{\partial R_h}$, $\frac{d\lambda_5}{dt}=-\frac{\partial H}{\partial S_m}$, $\frac{d\lambda_6}{dt}=-\frac{\partial H}{\partial E_m}$ and $\frac{d\lambda_7}{dt}=-\frac{\partial H}{\partial I_m}$, $\frac{d\lambda_8}{dt}=-\frac{\partial H}{\partial S_e}$, $\frac{d\lambda_9}{dt}=-\frac{\partial H}{\partial I_e}$, the adjoint system is given by

(49)

$$
\begin{aligned}
\dot{\lambda_1} &= \frac{(1+I_mk)\lambda_1\mu+(-1+c_1(t))I_m\alpha_1(-\lambda_1+\lambda_2)\rho}{1+I_mk}\\
\dot{\lambda_2} &= -W_1+\beta_1(\lambda_2-\lambda_3)+\lambda_2\mu\\
\dot{\lambda_3} &= -W_2+d\lambda_3+\gamma\lambda_3+bc_2(t)(\lambda_3-\lambda_4)-\gamma\lambda_4+\lambda_3\,\mu-(-1+c_1(t))S_m\alpha_2(\lambda_5-\lambda_6)\rho\\
\dot{\lambda_4} &= -\delta\lambda_1-\lambda_4(-\delta-\mu)\\
\dot{\lambda_5} &= -(1-c_1(t))I_h\alpha_2\lambda_6\rho-\lambda_5(-c_3(t)p-\xi-(1-c_1(t))I_h\alpha_2\rho)\\
\dot{\lambda_6} &= -W_3-\beta_2\lambda_7-\lambda_6(-c_3(t)p-\beta_2-\xi)\\
\dot{\lambda_7} &= \frac{-(1+I_mk)^2(W_4+\pi\theta(-\lambda_8+\lambda_9)-\lambda_7(c_3(t)p+\,\xi))-(-1+c_1(t))S_h\alpha_1(\lambda_1-\lambda_2)\rho}{(1+I_mk)^2}\\
\dot{\lambda_8} &= -\lambda_8(-c_3(t)p-\phi)-\lambda_5\phi\\
\dot{\lambda_9} &= -W_5-\lambda_9(-c_3(t)p-\phi)-\lambda_7\phi
\end{aligned}
$$

with the conditions for transversality provided by $\lambda_i(t_f)=0$ for $i=1$ to 9. Using the optimality conditions $\frac{\partial H}{\partial c_1}=0$, $\frac{\partial H}{\partial c_2}=0$, $\frac{\partial H}{\partial c_3}=0$, we get, $c_1^*=\frac{(I_mS_h\alpha_1(-\lambda_1+\lambda_2)+I_hS_m\alpha_2(-\lambda_5+\lambda_6)+I_hI_mkS_m\alpha_2(-\lambda_5+\lambda_6))\rho]}{(1+I_mk)W_6}$,

$c_2^* = \frac{bI_h(\lambda_3-\lambda_4)}{W_7}$, $c_3^* = \frac{p(S_m\lambda_5+E_m\lambda_6+I_m\lambda_7+S_e\lambda_8+I_e\lambda_9)}{W_8}$. Since $0 \le c_i \le 1$, we get,

(50)

$$c_1^* = \min\{\max\{0, \frac{(I_m S_h \alpha_1(-\lambda_1+\lambda_2) + I_h S_m \alpha_2(-\lambda_5+\lambda_6) + I_h I_m k S_m \alpha_2(-\lambda_5+\lambda_6))\rho]}{(1+I_m k)W_6}\}, 1\}$$

$$c_2^* = \min\{\max\{0, \frac{bI_h(\lambda_3-\lambda_4)}{W_7}\}, 1\}$$

$$c_3^* = \min\{\max\{0, \frac{p(S_m\lambda_5+E_m\lambda_6+I_m\lambda_7+S_e\lambda_8+I_e\lambda_9)}{W_8}\}, 1\}$$

Using (46), (49) and (50), the optimality system is given by

$$\dot{S_h} = \Omega - \frac{\rho(1-c_1^*(t))\alpha_1 I_m S_h}{1+kI_m} - \mu S_h + \delta R_h,\ \dot{E_h} = \frac{\rho(1-c_1^*(t))\alpha_1 I_m S_h}{1+kI_m} - (\beta_1+\mu)E_h,$$

$$\dot{I_h} = \beta_1 E_h - (\gamma + d + \mu + bc_2^*(t))I_h,\ \dot{R_h} = (\gamma + bc_2^*(t))I_h - (\delta+\mu)R_h$$

$$\dot{S_m} = \phi S_e - \rho(1-c_1^*(t))\alpha_2 I_h S_m - (\xi + pc_3^*(t))S_m,\ \dot{E_m} = \rho(1-c_1^*(t))\alpha_2 I_h S_m - (\beta_2+\xi+pc_3^*(t))E_m$$

$$\dot{I_m} = \beta_2 E_m + \phi I_e - (\xi + pc_3^*(t))I_m,\ \dot{S_e} = \Psi - \theta\pi I_m - (\phi + pc_3^*(t))S_e, \dot{I_e} = \theta\pi I_m - (\phi + pc_3^*(t))I_e$$

$$\dot{\lambda_1} = \frac{(1+I_m k)\lambda_1\mu + (1-c_1^*(t))I_m\alpha_1(\lambda_1-\lambda_2)\rho}{1+I_m k},\ \dot{\lambda_2} = \beta_1(\lambda_2-\lambda_3) + \lambda_2\mu - W_1$$

$$\dot{\lambda_3} = d\lambda_3 + \gamma\lambda_3 + bc_2^*(t)(\lambda_3-\lambda_4) + \lambda_3\ \mu + (1-c_1^*(t))S_m\alpha_2(\lambda_5-\lambda_6)\rho - W_2 - \gamma\lambda_4$$

$$\dot{\lambda_4} = \lambda_4(\delta+\mu) - \delta\lambda_1,\ \dot{\lambda_5} = \lambda_5(c_3^*(t)p + \xi + (1-c_1^*(t))I_h\alpha_2\rho) - (1-c_1^*(t))I_h\alpha_2\lambda_6\rho$$

$$\dot{\lambda_6} = \lambda_6(c_3^*(t)p + \beta_2 + \xi) - W_3 - \beta_2\lambda_7,\ \dot{\lambda_8} = \lambda_8(c_3^*(t)p+\phi) - \lambda_5\phi,\ \dot{\lambda_9} = \lambda_9(c_3^*(t)p+\phi) - \lambda_7\phi - W_5$$

$$\dot{\lambda_7} = \frac{(1+I_m k)^2(\pi\theta(\lambda_8-\lambda_9) + \lambda_7(c_3^*(t)p + \ \xi) - W_4) + (1-c_1^*(t))S_h\alpha_1(\lambda_1-\lambda_2)\rho}{(1+I_m k)^2}$$

subject to the conditions (2) and $\lambda_i(t_f) = 0$ for $i = 1$ to 9. □

9. Numerical Analysis and Simulation

9.1. Numerical analysis of stability theorems. In this section, simulation tests were performed to confirm the conclusions reached through analysis. Simulations have been performed on the proposed dengue model (1) to show local and global stability of the computed equilibrium points. For $R_0 < 1$ and $R_0 > 1$, the parameter values are chosen from table(5) and table(6), respectively.

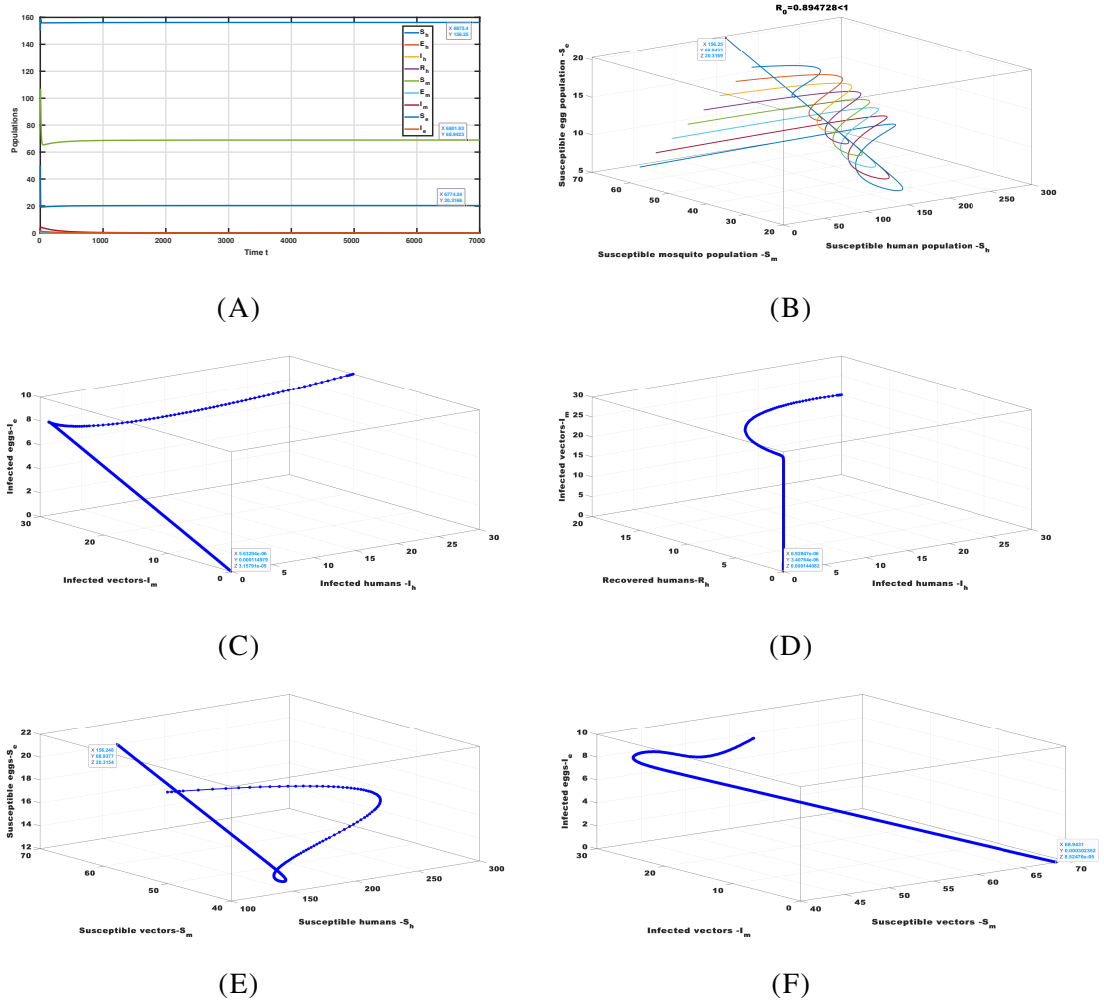

FIGURE 10. (A) The LAS of Q_0 of the dengue system (1) for $R_0 < 1$, (B) GAS of Q_0 shown in $(S_h - S_m - S_e)$ space for $R_0 < 1$, (C) The 3 D view of the convergence of the Infected human population (I_h), Infected vectors population (I_m) and infected egg population (I_e) towards Q_0 when $R_0 < 1$, (D) The 3 D view of the convergence of the Infected human population (I_h), Recovered human population (R_h) and infected vector population (I_m) towards Q_0 when $R_0 < 1$, (E) The 3 D view of the convergence of susceptible human population (S_h), susceptible vectors population (S_m) and susceptible egg population (S_e) towards Q_0 when $R_0 < 1$, (F) The 3 D view of the convergence of susceptible vector population (S_m), Infected vectors population (I_m) and infected egg population (I_e) towards Q_0 when $R_0 < 1$

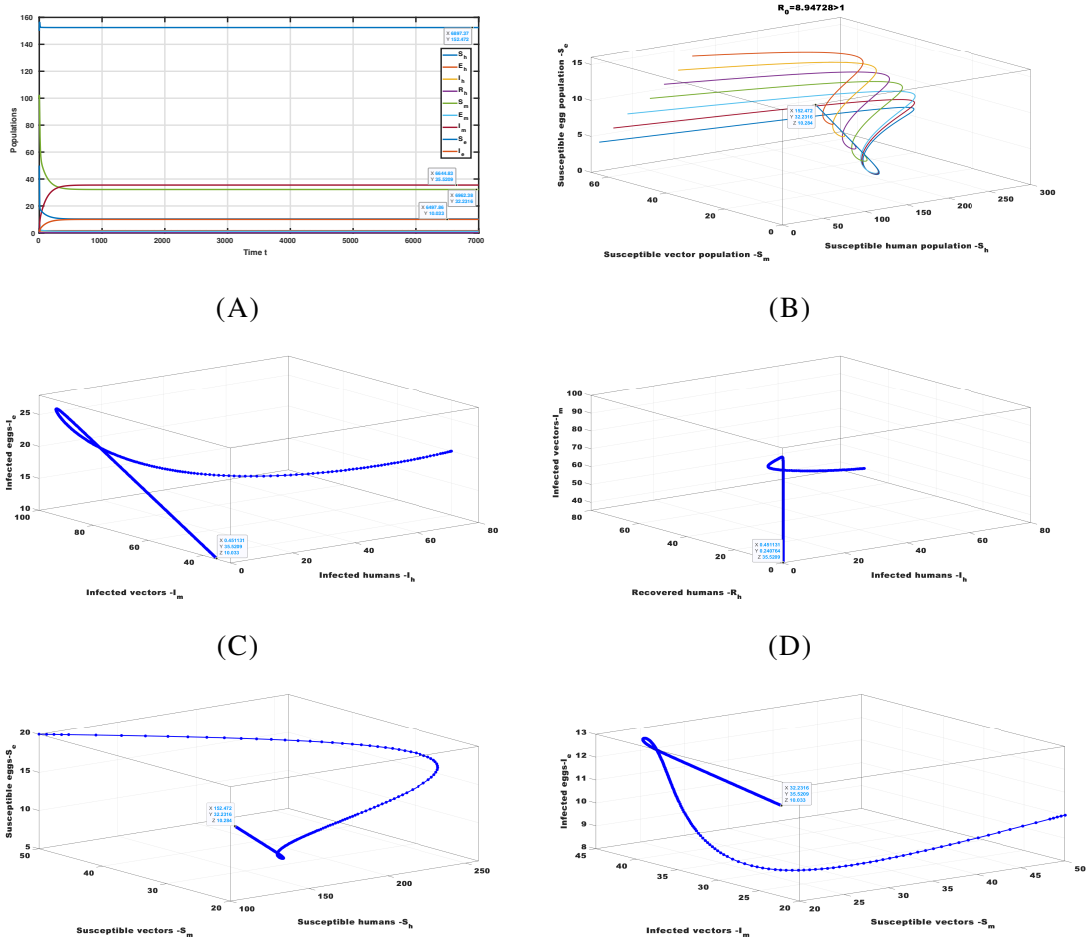

FIGURE 11. (A) The LAS of Q_1 of the dengue system (1) for $R_0 > 1$, (B) GAS of Q_1 shown in $(S_h - S_m - S_e)$ space for $R_0 > 1$, (C) The 3 D view of the convergence of the Infected human population (I_h), Infected vectors population (I_m) and infected egg population (I_e) towards Q_1 when $R_0 > 1$, (D) The 3 D view of the convergence of the Infected human population (I_h), Recovered human population (R_h) and infected vector population (I_m) towards Q_1 when $R_0 > 1$, (E) The 3 D view of the convergence of susceptible human population (S_h), susceptible vectors population (S_m) and susceptible egg population (S_e) towards Q_1 when $R_0 > 1$, (F) The 3 D view of the convergence of susceptible vector population (S_m), Infected vectors population (I_m) and infected egg population (I_e) towards Q_1 when $R_0 > 1$

The DFE point $Q_0(S_h^0, E_h^0, I_h^0, R_h^0, S_m^0, E_m^0, I_m^0, S_e^0, I_e^0)$ whose stability both global and local has been numerically simulated and depicted in figure (10). The DFE point is found to be Q_0(156.25, 0, 0, 0, 68.9434, 0, 0, 20.3169, 0) and $R_0 = 0.894728 < 1$ using table (5). For initial conditions of state variables near the equilibrium point Q_0 in Θ, it is seen from the figure (10)(A) that $\lim_{t\to\infty} S_h(t) = S_h^0 = 156.25$, $\lim_{t\to\infty} E_h(t) = E_h^0 = 0$, $\lim_{t\to\infty} I_h(t) = I_h^0 = 0$, $\lim_{t\to\infty} R_h(t) = R_h^0 = 0$, $\lim_{t\to\infty} S_m(t) = S_m^0 = 68.9434$, $\lim_{t\to\infty} E_m(t) = E_m^0 = 0$, $\lim_{t\to\infty} I_m(t) = I_m^0 = 0$, $\lim_{t\to\infty} S_e(t) = S_e^0 = 20.3169$, $\lim_{t\to\infty} I_e(t) = I_e^0 = 0$ when ever the initial conditions are chosen in Θ. The necessary and sufficient condition in theorem (3), namely $B_1 = 1.70659 > 0$, $B_2 = 1.03521 > 0$, $B_3 = 0.262404 > 0$, $B_4 = 0.0237132 > 0$, $B_5 = 0.0000198898 > 0$, $B_1B_2B_3 - B_3^2 - B_1^2B_4 = 0.325664 > 0$ and $(B_1B_4 - B_5)(B_1B_2B_3 - B_3^2 - B_1^2B_4) - B_5(B_1B_2 - B_3)^2 - B_1B_5^2 = 0.0131277 > 0$ are satisfied. Hence Q_0 is LAS in Θ as per the theorem (3). According to figure (10)(B), the solution for the initial conditions on the state variables $S_h(t)$, $S_m(t)$ and $S_e(t)$ in Θ_1 is $(S_h(t), S_m(t), S_e(t))$ $\to (S_h^0, S_m^0, S_e^0) = (156.25, 68.9434, 20.3169)$ as t $\to \infty$. With the initial conditions in Θ_1, this convergence may be confirmed for all feasible ordered triples out of the nine state variables. As per theorem (5), Q_0 is GAS in Θ_1 when $R_0 > 1$.

From figure (10)(C), it is noticed that the populations $I_h(t)$,$I_m(t)$ and I_e converges to $I_h^0 = 0$, $I_m^0 = 0$ and $I_e^0 = 0$ respectively as $t \to \infty$ whenever the initial points of state variables belongs to Θ_1. From the figures (10)(D), (10)(E), (10)(F), it is seen that the state variables $(I_h(t), R_h(t), I_m(t)) \to (I_h^0(t), R_h^0(t), I_m^0(t)) = (0,0,0)$, $(S_h(t), S_m(t), S_e(t)) \to (S_h^0(t), S_m^0(t), S_e^0(t)) = (156.25, 68.9434, 68.9434)$ and $(S_m(t), I_m(t), I_e(t)) \to (S_m^0(t), I_m^0(t), I_e^0(t)) = (68.9434, 0, 0)$ as $t \to \infty$ respectively whenever the initial populations belong to Θ_1.

The global and local stability of the EE point $Q_1(S_h^*, E_h^*, I_h^*, R_h^*, S_m^*, E_m^*, I_m^*, S_e^*, I_e^*)$ has been simulated numerically and shown in figure (11). The EE point is found as Q_1(152.472, 1.66891, 0.451144, 0.240764, 32.2316, 1.19083, 35.5209, 10.284, 10.033) and $R_0 = 8.94728 > 1$ using the values of parameter from table (6). Hence for different initial conditions coresponding to state variables near the equilibrium point Q_1 in Υ, it is seen from the figure (11)(A) that $\lim_{t\to\infty} S_h(t) = S_h^* = 152.472$, $\lim_{t\to\infty} E_h(t) = E_h^* = 1.66891$, $\lim_{t\to\infty} I_h(t) = I_h^* = 0.451144$, $\lim_{t\to\infty} R_h(t) = R_h^* = 0.240764$, $\lim_{t\to\infty} S_m(t) = S_m^* = 32.2316$, $\lim_{t\to\infty} E_m(t) = E_m^* = 1.19083$,

$\lim_{t\to\infty} I_m(t) = I_m^* = 35.5209$, $\lim_{t\to\infty} S_e(t) = S_e^* = 10.284$, $\lim_{t\to\infty} I_e(t) = I_e^* = 10.033$. In addition, the necessary and sufficient condition as stated in theorem (6), namely for $b_1 = 3.12409$, $b_2 = 3.98792$, $b_3 = 2.66994$, $b_4 = 1.00525$, $b_5 = 0.21396$, $b_6 = 0.0249967$, $b_7 = 0.00147221$,we get $|H_1| = 3.12409 > 0$, $|H_2| = 9.78867 > 0$, $|H_3| = 16.9924 > 0$, $|H_4| = 10.1056 > 0$, $|H_5| = 1.27002 > 0$, $|H_6| = 0.018925 > 0$, $|H_7| = 0.0000278617 > 0$, $|H_8| = 9.39119 \times 10^{-10} > 0$ are satisfied. Hence Q_1 is LAS in Υ as per the theorem (6). From figure (11)(B), it is found that for any initial conditions of state variables $S_h(t)$, $S_m(t)$ and $S_e(t)$ in Υ, the solutions $(S_h(t), S_m(t), S_e(t)) \to (S_h^*, S_m^*, S_e^*) = (152.472, 32.2316, 10.284)$ as $t \to \infty$. This property of convergence can be checked for all ordered triples of state variables with the initial conditions in Υ. As per the results of theorem (7), it is found that Q_1 is GAS in Υ when $R_0 > 1$. From figure (11)(C), it is seen that the populations $I_h(t)$,$I_m(t)$ and I_e converges to $I_h^* = 0.451144$, $I_m^* = 35.5209$ and $I_e^* = 10.033$ respectively as $t \to \infty$ when the initial state variables belong to Υ. Similarly from the figures (11)(D), (11)(E), (11)(F), it is seen that the state variables $(I_h(t), R_h(t), I_m(t)) \to (I_h^*(t), R_h^*(t), I_m^*(t)) = (0.451144, 0.240764, 35.5209)$, $(S_h(t), S_m(t), S_e(t)) \to (S_h^*(t), S_m^*(t), S_e^*(t)) = (152.472, 32.2316, 10.284)$ and $(S_m(t), I_m(t), I_e(t)) \to (S_m^*(t), I_m^*(t), I_e^*(t))$= (32.2316, 35.5209, 10.033) as $t \to \infty$ respectively whenever the initial populations belong to Υ.

TABLE 5. parameter values for constructing figure (10)

Parameter	Ω	Ψ	α_1	α_2	β_1	β_2	θ	ρ	ϕ	μ	γ	d	b	ξ	p	π	k	δ	c_1	c_2	c_3
Value	10	10	0.0165	0.165	0.153	0.165	0.513	0.0165	0.452	0.064	0.271	0.201	0.163	0.093	0.201	0.271	1	0.5	0.103	0.184	0.2

TABLE 6. parameter values for constructing figure (11)

parameters	Ω	Ψ	α_1	α_2	β_1	β_2	θ	ρ	ϕ	μ	γ	d	b	ξ	p	π	k	δ	c_1	c_2	c_3
values	10	10	0.0165	0.165	0.153	0.165	0.513	0.165	0.452	0.064	0.271	0.201	0.163	0.093	0.201	0.271	1	0.5	0.103	0.184	0.2

9.2. Numerical analysis of control strategies. The system (1) is analysed numerically using the parameters as in table (7). It is assumed that the recruitment rate of human population (Ω) and the recruitment rate of Aedes Aegypti mosquitoes eggs per day (Ψ) are 500. The disease transmission rates for human and vector populations, namely α_1 and α_2 are assumed as 10^{-6}.

The incubation period for dengue virus is of 5-7 days, the progression rate from exposed to infected human population (β_1) is assumed between 0.14-0.2, say 0.17. The extrinsic incubation period say the progression rate from exposed to infected female Aedes Aegypti mosquito population is 8-12 days [1]. Hence the progression rate (β_2) from exposed to infected compartment is assumed between 0.08-0.125 say 0.1. The mean life time of humans is assumed as 68 years and hence the human population natural mortality rate (μ) is assumed to be $\frac{1}{68\times 365}$ which is approximately 4×10^{-5}. The adult mosquitoes can live up to one month [76]. Hence the natural mortality rate of adult mosquito (ξ) is assumed as 0.04. Symptoms of dengue typically last 2–7 days and most people will recover after about a week [76]. Hence the natural recovery rate of hosts from the infection (γ) is assumed as 0.14. The death rate due to disease (d) for humans is assumed as 10^{-5}. The humans who get recovered from dengue disease of a particular serotype virus attains life time immunity but after 2 to 3 months reinfection with different serotype is possible [77]. Hence the reinfection rate (δ) is assumed to be between 0.0111-0.0167 say 0.01 approximately. The saturation factor (k) is assumed as zero. The effectiveness of the control c_2 say b is assumed as 0.5. The effectiveness of the control c_3 say p is assumed as 0.7. A mosquito egg develops into an adult mosquito in 9 to 12 days [78]. Hence the development rate of Aedes Aegypti mosquito eggs (ϕ) is assumed to be between 0.08-0.11 say 0.08. The vertical transmission rate (π) of dengue virus in Aedes Aegypti mosquitoes is assumed to be 10^{-6}. The effective biting rate of mosquitoes ρ is assumed as 0.08

The figures 12 to 23 are constructed using the parameter estimated values as in table (7). The initial population sizes are assumed to be $S_h(0)=10^7$, $E_h(0)=50$, $I_h(0)=10$, $R_h(0)=10$, $S_m(0)=10^6$, $E_m(0)=50$, $I_m(0)=10$, $S_e(0)=10^4$, $I_e(0)=5$. The weights for the optimal control analysis is assumed to be $W_i=0.01$ and $W_j=100$ for $i=1$ to 5 and $j=6$ to 8.

Figures (12)(A) and (12)(B) show that increasing disease transmission rates (α_1 and α_2) in human and vector populations, respectively, increases the basic reproduction number relative to unity. Hence, the endemic equilibrium is more stable, and the disease persists in society for an extended period.

TABLE 7. The estimated parameter values of system (1)

Parameters	**values**	**source**
Ω	500	Assumed
Ψ	500	Assumed
α_1	10^{-6}	Assumed
α_2	10^{-6}	Assumed
β_1	0.17	[1]
β_2	0.1	[1]
μ	4×10^{-5}	Assumed
ξ	0.04	[76]
γ	0.14	[76]
d	10^{-5}	Assumed
δ	0.01	[77]
k	0	Assumed
b	0.5	Assumed
p	0.7	Assumed
ϕ	0.08	[78]
θ	500	Assumed
π	10^{-6}	Assumed
ρ	0.08	Assumed

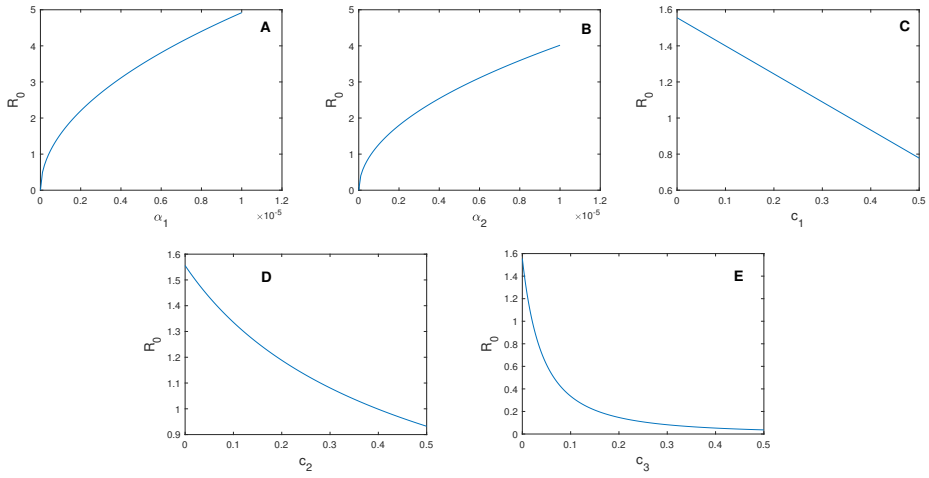

FIGURE 12. Variation of Basic Reproduction Number R_0 with: (A) Human disease transmission rate, α_1; (B) Vector disease transmission rate, α_2; (C) Protection control c_1; (D) Treatment control for human infection, c_2; (E) Insecticide spray control against mosquitoes, c_3. Parameter values as per Table (7).

Figures (12)(C)-(12)(E) show that a gradual increase in the rates of protection controls (c_1), treatment controls (c_2), and insecticide spray controls (c_3) against mosquitoes reduces the basic reproduction number under unity, stabilizing the disease-free equilibrium and eradicating the disease from society.

Figures (13)(A)-(13)(D) show that as disease transmission rates (α_1 and α_2) increase in the human and vector populations, respectively, so do the infected populations (I_h and I_m) in the human and vector populations.

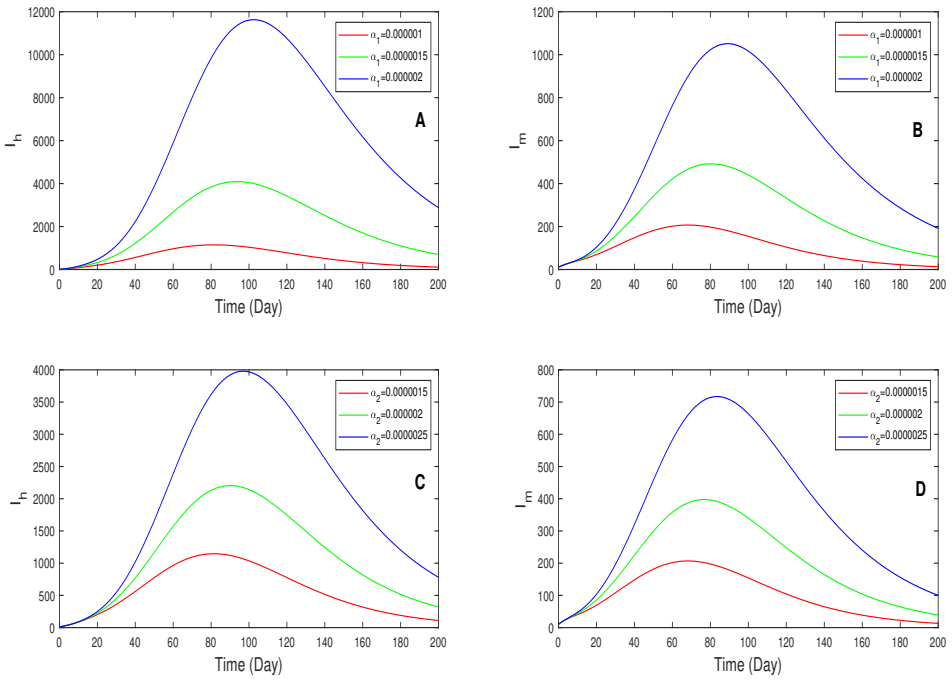

FIGURE 13. Time series graphs of infected populations I_h and I_m for varying human disease transmission rate, α_1, and vector disease transmission rate, α_2. Parameter values from Table (7).

It is found from figures (14)(A)-(14)(F) that the increase in the rate of the protection control c_1, treatment control c_2 and insecticide spray control c_3, results in a decrease in the infected populations, namely I_h and I_m among the human and vector populations, respectively.

It is found from figures (15)(A)-(15)(B) that the increase in the saturation factor k, results in a decrease in the infected populations, namely I_h and I_m among the human and vector populations, respectively.

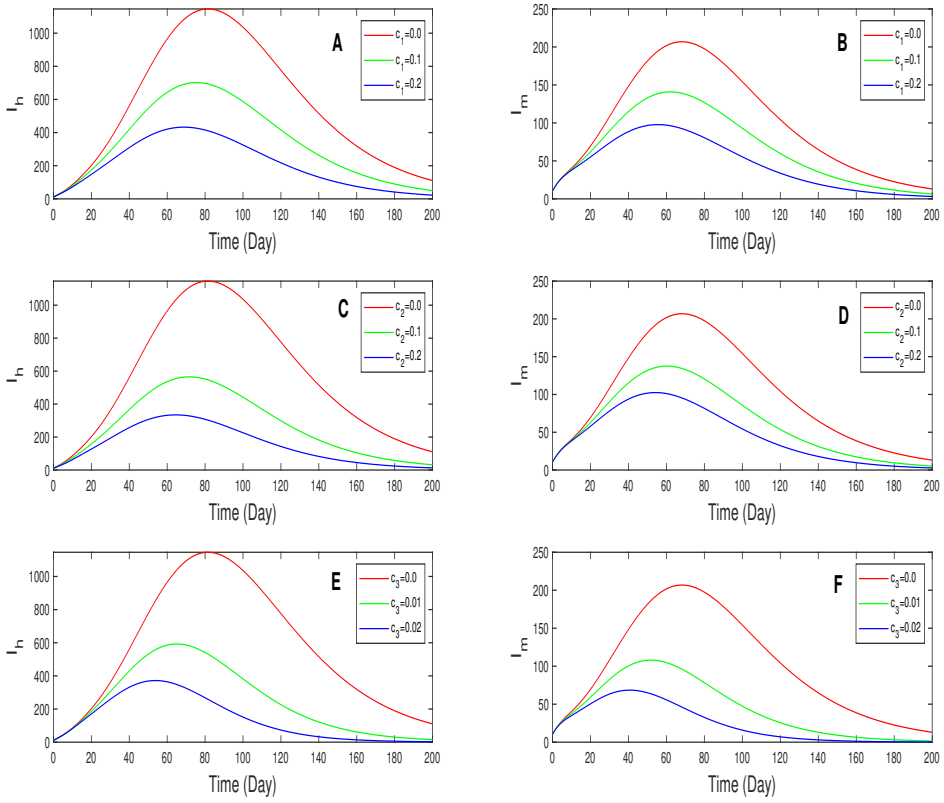

FIGURE 14. Time series graphs of infected populations I_h and I_m for different values of protection controls (c_1), treatment controls for humans infected with either serotype virus (c_2), and insecticide spray control against mosquitoes (c_3), with parameter values as assumed from Table (7).

Figures (16)(A)- (16)(C) clearly show that controls, specifically protection controls (c_1), treatment controls for humans infected with either serotype virus (c_2), and mosquito insecticide spray control (c_3), should be implemented early on to control the rapid spread of dengue disease.

From figure(17), it is obvious that when all controls are applied simultaneously, there is a rapid decrease in the infected populations I_h and I_m of human and vector populations, respectively.

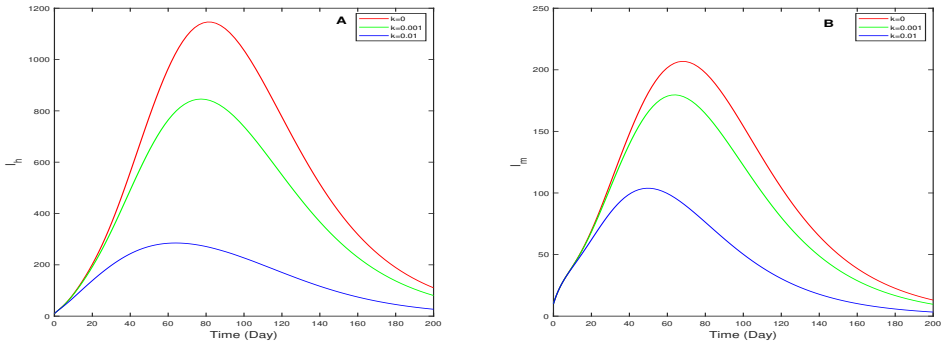

FIGURE 15. Time series graphs of the infected populations I_h and I_m for various values of k.

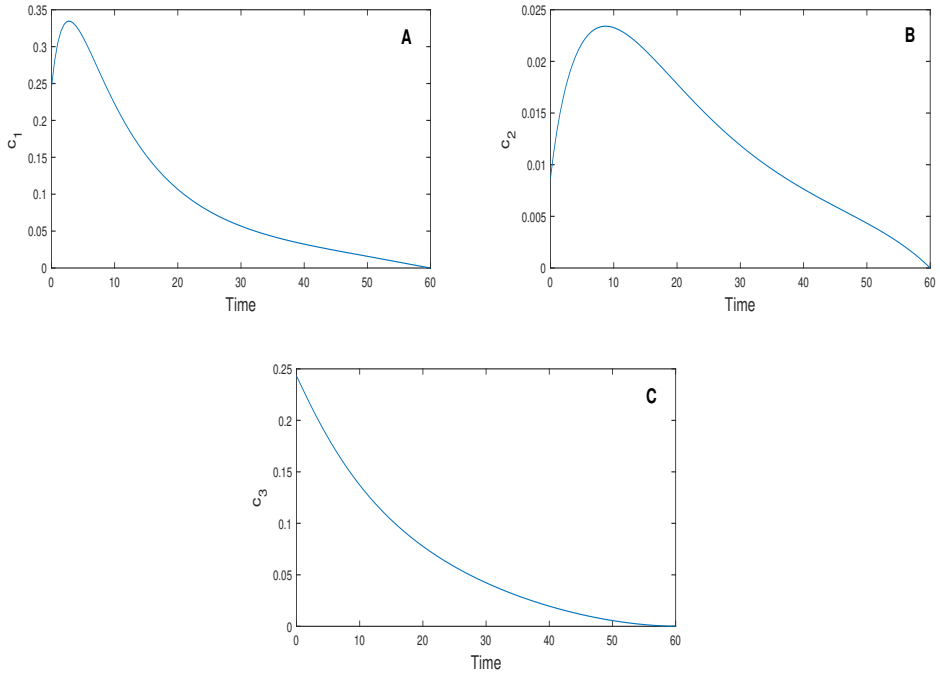

FIGURE 16. Time series of the Optimal controls c_1, c_2 and c_3.

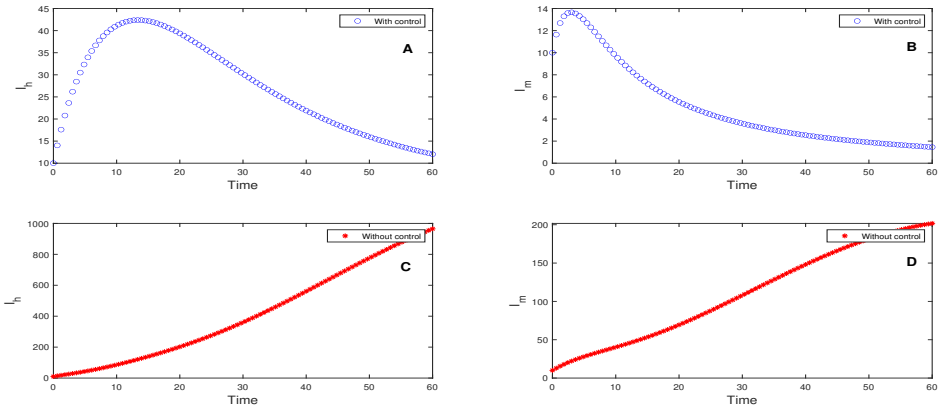

FIGURE 17. Time series: (A) I_h with all controls, (B) I_h without controls, (C) I_m without controls. Parameters from Table (7).

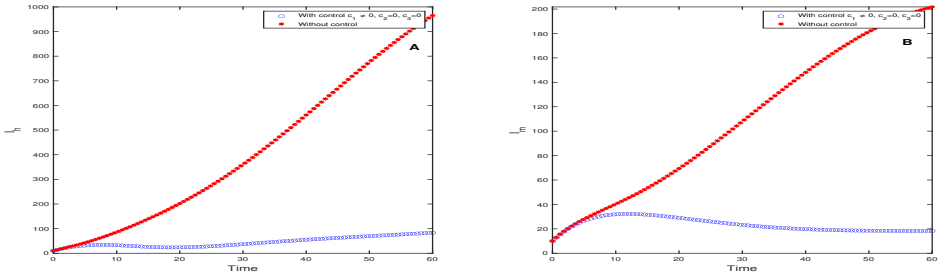

FIGURE 18. Time series of the infected population (A) I_h with implementing the protection control, c_1, (B) I_m with implementing the protection control, c_1 with the parameter values as assumed from table(7) .

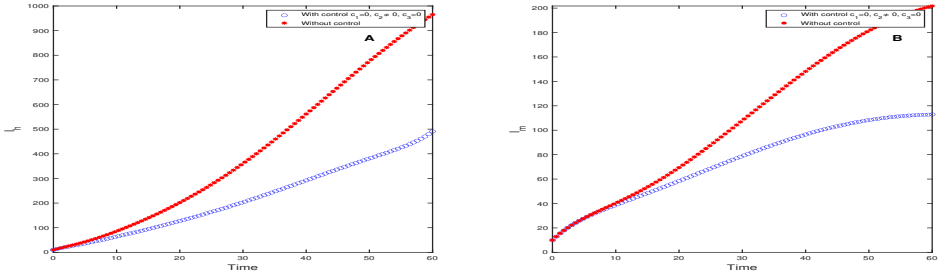

FIGURE 19. Time series of the infected population (A) I_h with implementing the treatment control, c_2, (B) I_m with implementing the treatment control, c_2 with the parameter values as assumed from table(7).

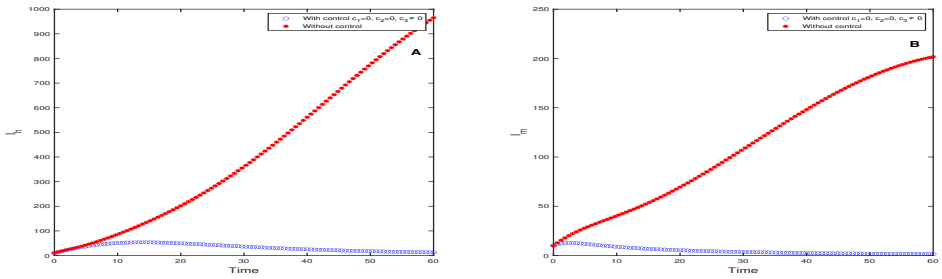

FIGURE 20. Time series of the infected population, (A) I_h with implementing the insecticide spray control, c_3, (B) I_m with implementing the insecticide spray control, c_3 with the parameter values as assumed from table(7).

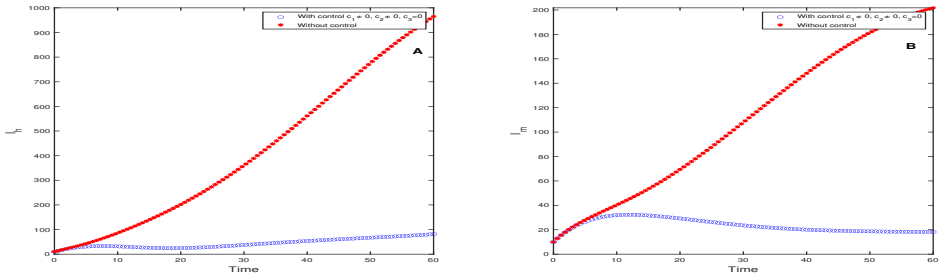

FIGURE 21. Time series of infected populations with protection control c_1 and treatment control c_2: (A) I_h, (B) I_m. Parameter values as per Table (7).

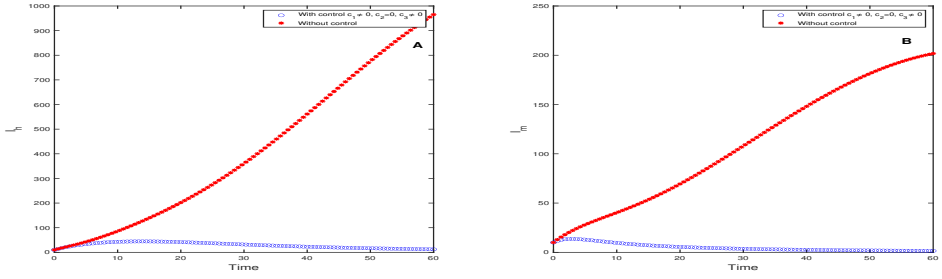

FIGURE 22. Time series of infected populations: (A) I_h with protection control c_1 and insecticide spray control c_3, (B) I_m with protection control c_1 and insecticide spray control c_3. Parameter values from Table (7).

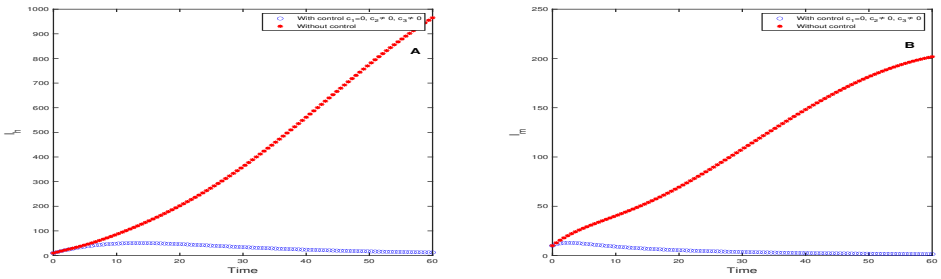

FIGURE 23. Time series of infected populations: (A) I_h with treatment control c_2 and insecticide spray control c_3, (B) I_m with treatment control c_2 and insecticide spray control c_3. Parameter values from Table (7).

The numerical analysis of optimal control strategies for managing and mitigating dengue disease presents a comprehensive assessment of various intervention measures aimed at curbing the rapid spread of this debilitating disease. Dengue, a mosquito-borne viral infection, poses a significant public health challenge worldwide, making effective control strategies crucial in reducing its impact on human populations. This section examines the outcomes of employing protection controls (c_1), treatment controls for infected humans (c_2), and mosquito insecticide spray control (c_3), both independently and in combination, using the dynamic simulations depicted in the provided figures.

Effectiveness of Individual Control Strategies: Protection Control (c_1):

Figure (18) illustrates the impact of implementing protection control measures. The time series graph demonstrates an apparent reduction in the infected human population (I_h) when protection controls are in place. By imposing quarantine measures, vaccinations, or other means to shield susceptible individuals from exposure, the progression of the disease is notably hindered. This emphasizes the significance of preemptive measures to protect vulnerable populations from contracting the virus.

Treatment Control for Humans Infected with the Dengue Virus (c_2):

The utilization of treatment control strategies is highlighted in figure (19). This graph unveils a decrease in the infected human population (I_h) due to the timely and effective treatment of individuals infected with the dengue virus. The treatment controls contribute significantly to

curtailing the spread of the disease within the human population.

Mosquito Insecticide Spray Control (c_3):

The impact of mosquito insecticide spray control is depicted in figure (20). The time series graph reveals a decline in the infected mosquito population (I_m) due to targeted insecticide applications. Targeting the vectors responsible for disease transmission disrupts the mosquito-human transmission cycle, thereby reducing the overall disease burden.

Synergistic Effects of Combined Control Strategies:

Figures (21), (22), and (23) explore the synergistic impact of employing two control strategies simultaneously. These combinations demonstrate enhanced efficacy in disease control compared to individual strategies.

Protection Control (c_1) + Treatment Control (c_2):

Figure (21) showcases the outcomes of combining protection and treatment controls. The infected human population (I_h) experiences a pronounced decline, reinforcing that safeguarding susceptible individuals and treating those infected are complementary strategies for effective disease management. *Protection Control (c_1) + Insecticide Spray Control (c_3):*

The combination of protection and insecticide spray controls is investigated in figure (22). This combination significantly reduces both infected human and mosquito populations (I_h and I_m), underscoring the importance of interrupting both human-to-human and human-to-mosquito transmission.

Treatment Control (c_2) + Insecticide Spray Control (c_3):

Figure (23) illustrates the dynamic impact of employing treatment and insecticide spray controls in tandem. The time series graph demonstrates a substantial reduction in infected populations (I_h and I_m), indicating the effectiveness of targeting both vectors and infected individuals.

Conclusive Insights:

Collectively, the presented numerical analysis underscores the significance of early implementation of control strategies to mitigate the rapid spread of dengue disease effectively. The synergistic effects observed in the combined strategy emphasize the importance of multifaceted

approaches to combat this complex disease. The findings of this analysis provide valuable insights for policymakers, healthcare professionals, and researchers striving to formulate comprehensive and targeted strategies for dengue disease control, ultimately contributing to improved public health outcomes on a global scale.

10. Conclusion

In this research, a mathematical model for Dengue disease transmission with a saturated incidence function among the human population and a bi-linear transmission function among vectors has been formulated and studied. The vector population was divided into adult and egg populations and considered to have vertical transmission among vector populations. The human population reinfection component was added to the model. The fundamental properties of the system, like non-negativity and uniform boundedness of solutions of the model (1), were proved theoretically. The equilibrium points, namely the DFE and EE points, were found and analysed for their existence. The basic reproduction number was determined as the average number of new infections caused by one infected person in a population that is completely susceptible. The local and global stability of the equilibrium points is examined under particular conditions. By computing the various sensitivity indices of highly sensitive parameters relative to the basic reproduction number, the sensitivity analysis of the model is performed. According to bifurcation analysis, a stable endemic equilibrium coexists with an unstable disease-free equilibrium point, where the bifurcation parameter is the disease transmission rate of the human population (α_1). Forward bifurcation occurs at $R_0 = 1$. From an epidemiological point of view, the dengue disease persists in the host population for a very long period of time, as per the model (1). Parameter estimation is done, and used those values to perform simulations of the system. The optimal control problem is framed and analysed as the optimal system for the existence of optimal controls, namely protection control, treatment control, and insecticide spray control. The optimal controls are found theoretically and later simulated using the estimated parameter values. The simulation of the model using some assumed values verified the theoretically proven results for the stability analysis. The simulation of the optimal control model using the estimated values of parameters highlights the importance of implementing the optimal

controls together at the initial stage of the spread of dengue disease among the susceptible human population. The model is analysed with only three control strategies, and the model can be modified to investigate the control strategy of introducing a Wolbachia-affected female Aedes aegypti mosquito among the vector population with different serotype infections and analyse the disease transmission dynamics of the improved model.

CONFLICT OF INTERESTS

The authors declare that there is no conflict of interests.

REFERENCES

[1] Centers for Disease Control and Prevention, https://www.cdc.gov/dengue/healthcare-providers/clinical-presentation.html. Accessed: April 13, 2023.

[2] R. Taghikhani, O. Sharomi, A.B. Gumel, Dynamics of a two-sex model for the population ecology of dengue mosquitoes in the presence of Wolbachia, Math. Biosci. 328 (2020), 108426. https://doi.org/10.1016/j.mbs.2020.108426.

[3] J.J. Tewa, J.L. Dimi, S. Bowong, Lyapunov functions for a dengue disease transmission model, Chaos Solitons Fractals. 39 (2009), 936–941. https://doi.org/10.1016/j.chaos.2007.01.069.

[4] L. Cai, S. Guo, X. Li, M. Ghosh, Global dynamics of a dengue epidemic mathematical model, Chaos Solitons Fractals. 42 (2009), 2297–2304. https://doi.org/10.1016/j.chaos.2009.03.130.

[5] A.K. Srivastav, P.K. Tiwari, M. Ghosh, Modeling the impact of early case detection on dengue transmission: deterministic vs. stochastic, Stoch. Anal. Appl. 39 (2020), 434–455. https://doi.org/10.1080/07362994.2020.1804403.

[6] S.M. Garba, A.B. Gumel, M.R. Abu Bakar, Backward bifurcations in dengue transmission dynamics, Math. Biosci. 215 (2008), 11–25. https://doi.org/10.1016/j.mbs.2008.05.002.

[7] J. Li, Y. Lou, Characteristics of an epidemic outbreak with a large initial infection size, J. Biol. Dyn. 10 (2016), 366–378. https://doi.org/10.1080/17513758.2016.1205223.

[8] A.A. de los Reyes V, J.M.L. Escaner IV, Dengue in the Philippines: model and analysis of parameters affecting transmission, J. Biol. Dyn. 12 (2018), 894–912. https://doi.org/10.1080/17513758.2018.1535096.

[9] J.J. Thibodeaux, D. Nuñez, A. Rivera, A generalized within-host model of dengue infection with a non-constant monocyte production rate, J. Biol. Dyn. 14 (2020), 143–161. https://doi.org/10.1080/17513758.2020.1733678.

[10] M.C. Gómez, H.M. Yang, Mathematical model of the immune response to dengue virus, J. Appl. Math. Comput. 63 (2020), 455–478. https://doi.org/10.1007/s12190-020-01325-8.

[11] L. Esteva, C. Vargas, A model for dengue disease with variable human population, J. Math. Biol. 38 (1999), 220–240. https://doi.org/10.1007/s002850050147.

[12] R.A. Erickson, S.M. Presley, L.J.S. Allen, et al. A dengue model with a dynamic Aedes albopictus vector population, Ecol. Model. 221 (2010), 2899–2908. https://doi.org/10.1016/j.ecolmodel.2010.08.036.

[13] F.A.B. Coutinhoa, M.N. Burattinia, L.F. Lopeza, et al. Threshold conditions for a non-autonomous epidemic system describing the population dynamics of dengue, Bull. Math. Biol. 68 (2006), 2263–2282. https://doi.org/10.1007/s11538-006-9108-6.

[14] M. Borisov, G. Dimitriu, P. Rashkov, Modelling the host immune response to mature and immature dengue viruses, Bull. Math. Biol. 81 (2019), 4951–4976. https://doi.org/10.1007/s11538-019-00664-3.

[15] L.E. Lopez, A.M. Loaiza, G.O. Tost, A mathematical model for transmission of dengue, Appl. Math. Sci. 10 (2016), 345–355. https://doi.org/10.12988/ams.2016.510662.

[16] S.M. Garba, A.B. Gumel, M.R. Abu Bakar, Backward bifurcations in dengue transmission dynamics, Math. Biosci. 215 (2008), 11–25. https://doi.org/10.1016/j.mbs.2008.05.002.

[17] F. Bacani, S. Dimas, I.L. Freire, et al. Mathematical modelling for the transmission of dengue: Symmetry and travelling wave analysis, Nonlinear Anal.: Real World Appl. 41 (2018), 269–287. https://doi.org/10.1016/j.nonrwa.2017.10.013.

[18] S. Ottaviano, M. Sensi, S. Sottile, Global stability of SAIRS epidemic models, Nonlinear Anal.: Real World Appl. 65 (2022), 103501. https://doi.org/10.1016/j.nonrwa.2021.103501.

[19] O. Martin, Y. Fernandez-Diclo, J. Coville, et Equilibrium and sensitivity analysis of a spatio-temporal host-vector epidemic model, Nonlinear Anal.: Real World Appl. 57 (2021), 103194. https://doi.org/10.1016/j.nonrwa.2020.103194.

[20] Z. Feng, J.X. Velasco-Hernández, Competitive exclusion in a vector-host model for the dengue fever, J. Math. Biol.35 (1997), 523–544. https://doi.org/10.1007/s002850050064.

[21] P. Agarwal, R. Singh, A. ul Rehman, Numerical solution of hybrid mathematical model of dengue transmission with relapse and memory via Adam-Bashforth-Moulton predictor-corrector scheme, Chaos Solitons Fractals. 143 (2021), 110564. https://doi.org/10.1016/j.chaos.2020.110564.

[22] A. Abidemi, N.A.B. Aziz, Optimal control strategies for dengue fever spread in Johor, Malaysia, Computer Methods Progr. Biomed. 196 (2020), 105585. https://doi.org/10.1016/j.cmpb.2020.105585.

[23] S.A. Carvalho, S.O. da Silva, I. da C. Charret, Mathematical modeling of dengue epidemic: control methods and vaccination strategies, Theory Biosci. 138 (2019), 223–239. https://doi.org/10.1007/s12064-019-00273-7.

[24] L.S. Sepulveda-Salcedo, O. Vasilieva, M. Svinin, Optimal control of dengue epidemic outbreaks under limited resources, Stud. Appl. Math. 144 (2020), 185–212. https://doi.org/10.1111/sapm.12295.

[25] H.S. Rodrigues, M.T.T. Monteiro, D.F.M. Torres, Vaccination models and optimal control strategies to dengue, Math. Biosci. 247 (2014), 1–12. https://doi.org/10.1016/j.mbs.2013.10.006.

[26] S. Lee, C. Castillo-Chavez, The role of residence times in two-patch dengue transmission dynamics and optimal strategies, J. Theor. Biol. 374 (2015), 152–164. https://doi.org/10.1016/j.jtbi.2015.03.005.

[27] I. Ghosh, P.K. Tiwari, J. Chattopadhyay, Effect of active case finding on dengue control: Implications from a mathematical model, J. Theor. Biol. 464 (2019), 50–62. https://doi.org/10.1016/j.jtbi.2018.12.027.

[28] H.S. Rodrigues, M.T.T. Monteiro, D.F.M. Torres, Bioeconomic perspectives to an optimal control dengue model, Int. J. Computer Math. 90 (2013), 2126–2136. https://doi.org/10.1080/00207160.2013.790536.

[29] A. Khatua, T.K. Kar, Dynamical behavior and control strategy of a dengue epidemic model, Eur. Phys. J. Plus. 135 (2020), 643. https://doi.org/10.1140/epjp/s13360-020-00654-8.

[30] A.A. Lashari, G. Zaman, Optimal control of a vector borne disease with horizontal transmission, Nonlinear Anal.: Real World Appl. 13 (2012), 203–212. https://doi.org/10.1016/j.nonrwa.2011.07.026.

[31] A. Abidemi, M.I. Abd Aziz, R. Ahmad, Vaccination and vector control effect on dengue virus transmission dynamics: Modelling and simulation, Chaos Solitons Fractals. 133 (2020), 109648. https://doi.org/10.1016/j.chaos.2020.109648.

[32] L. Xue, X. Ren, F. Magpantay, et al. Optimal control of mitigation strategies for dengue virus transmission, Bull Math Biol. 83 (2021), 8. https://doi.org/10.1007/s11538-020-00839-3.

[33] R. Jan, Y. Xiao, Effect of pulse vaccination on dynamics of dengue with periodic transmission functions, Adv. Differ. Equ. 2019 (2019), 368. https://doi.org/10.1186/s13662-019-2314-y.

[34] J. Llibre, R.D.S. Oliveira, C. Valls, Final evolutions for simplified multistrain/two-stream model for tuberculosis and dengue fever, Chaos Solitons Fractals. 118 (2019), 181–186. https://doi.org/10.1016/j.chaos.2018.11.022.

[35] T.T. Zheng, L.F. Nie, Modelling the transmission dynamics of two-strain Dengue in the presence awareness and vector control, J. Theor. Biol. 443 (2018), 82–91. https://doi.org/10.1016/j.jtbi.2018.01.017.

[36] M. Aguiar, S. Ballesteros, B.W. Kooi, et al. The role of seasonality and import in a minimalistic multi-strain dengue model capturing differences between primary and secondary infections: Complex dynamics and its implications for data analysis, J. Theor. Biol. 289 (2011), 181–196. https://doi.org/10.1016/j.jtbi.2011.08.043.

[37] L. Xue, H. Zhang, W. Sun, C. Scoglio, Transmission dynamics of multi-strain dengue virus with cross-immunity, Appl. Math. Comput. 392 (2021), 125742. https://doi.org/10.1016/j.amc.2020.125742.

[38] L. Esteva, C. Vargas, Coexistence of different serotypes of dengue virus, J. Math. Biol. 46 (2003), 31–47. https://doi.org/10.1007/s00285-002-0168-4.

[39] M. Aguiar, B. Kooi, N. Stollenwerk, Epidemiology of dengue fever: a model with temporary cross-immunity and possible secondary infection shows bifurcations and chaotic behaviour in wide parameter regions, Math. Model. Nat. Phenom. 3 (2008), 48–70. https://doi.org/10.1051/mmnp:2008070.

[40] L. Xue, H. Zhang, W. Sun, et al. Transmission dynamics of multi-strain dengue virus with cross-immunity, Appl. Math. Comput. 392 (2021), 125742. https://doi.org/10.1016/j.amc.2020.125742.

[41] A.M.C. Brito da Cruz, H.S. Rodrigues, Personal protective strategies for dengue disease: Simulations in two coexisting virus serotypes scenarios, Math. Computers Simul. 188 (2021), 254–267. https://doi.org/10.1016/j.matcom.2021.04.002.

[42] H. Song, D. Tian, C. Shan, Modeling the effect of temperature on dengue virus transmission with periodic delay differential equations, Math. Biosci. Eng. 17 (2020), 4147–4164. https://doi.org/10.3934/mbe.2020230.

[43] M. Zhu, Z. Lin, L. Zhang, The asymptotic profile of a dengue model on a growing domain driven by climate change, Appl. Math. Model. 83 (2020), 470–486. https://doi.org/10.1016/j.apm.2020.03.006.

[44] N.I. Hamdan, A. Kilicman, The development of a deterministic dengue epidemic model with the influence of temperature: A case study in Malaysia, Appl. Math. Model. 90 (2021), 547–567. https://doi.org/10.1016/j.apm.2020.08.069.

[45] B. Zheng, M. Tang, J. Yu, J. Qiu, Wolbachia spreading dynamics in mosquitoes with imperfect maternal transmission, J. Math. Biol. 76 (2017), 235–263. https://doi.org/10.1007/s00285-017-1142-5.

[46] Y. Li, L. Liu, The impact of Wolbachia on dengue transmission dynamics in an SEI-SIS model, Nonlinear Anal.: Real World Appl. 62 (2021), 103363. https://doi.org/10.1016/j.nonrwa.2021.103363.

[47] L. Xue, C.A. Manore, P. Thongsripong, J.M. Hyman, Two-sex mosquito model for the persistence ofWolbachia, J. Biol. Dyn. 11 (2016), 216–237. https://doi.org/10.1080/17513758.2016.1229051.

[48] H. Hughes, N.F. Britton, Modelling the use of wolbachia to control dengue fever transmission, Bull. Math. Biol. 75 (2013), 796–818. https://doi.org/10.1007/s11538-013-9835-4.

[49] T.A. McLennan-Smith, G.N. Mercer, Complex behaviour in a dengue model with a seasonally varying vector population, Math. Biosci. 248 (2014), 22–30. https://doi.org/10.1016/j.mbs.2013.11.003.

[50] K.F. Nipa, S.R.J. Jang, L.J.S. Allen, The effect of demographic and environmental variability on disease outbreak for a dengue model with a seasonally varying vector population, Math. Biosci. 331 (2021), 108516. https://doi.org/10.1016/j.mbs.2020.108516.

[51] E.A. Iboi, A.B. Gumel, Mathematical assessment of the role of Dengvaxia vaccine on the transmission dynamics of dengue serotypes, Math. Biosci. 304 (2018), 25–47. https://doi.org/10.1016/j.mbs.2018.07.003.

[52] S.M.A. Rahman, X. Zou, Modelling the impact of vaccination on infectious diseases dynamics, J. Biol. Dyn. 9 (2014), 307–320. https://doi.org/10.1080/17513758.2014.986545.

[53] M. Sriprom, P. Barbazan, I.M. Tang, Destabilizing effect of the host immune status on the sequential transmission dynamic of the dengue virus infection, Math. Computer Model. 45 (2007), 1053–1066. https://doi.org/10.1016/j.mcm.2006.09.011.

[54] W.E. Fitzgibbon, J.J. Morgan, G.F. Webb, et al. A vector-host epidemic model with spatial structure and age of infection, Nonlinear Anal.: Real World Appl. 41 (2018), 692–705. https://doi.org/10.1016/j.nonrwa.2017.11.005.

[55] A. Mishra, S. Gakkhar, Stage-structured transmission model incorporating secondary dengue infection, Differ. Equ. Dyn. Syst. 29 (2017), 569–584. https://doi.org/10.1007/s12591-017-0387-1.

[56] F. de A. Camargo, M. Adimy, L. Esteva, et al. Modeling the relationship between antibody-dependent enhancement and disease severity in secondary dengue infection, Bull. Math. Biol. 83 (2021), 85. https://doi.org/10.1007/s11538-021-00919-y.

[57] N. Anggriani, H. Tasman, M.Z. Ndii, et al. The effect of reinfection with the same serotype on dengue transmission dynamics, Appl. Math. Comput. 349 (2019), 62–80. https://doi.org/10.1016/j.amc.2018.12.022.

[58] A.K. Srivastav, M. Ghosh, Assessing the impact of treatment on the dynamics of dengue fever: A case study of India, Appl. Math. Comput. 362 (2019), 124533. https://doi.org/10.1016/j.amc.2019.06.047.

[59] P. Heidrich, Y. Jayathunga, W. Bock, et al. Prediction of dengue cases based on human mobility and seasonality–An example for the city of Jakarta, Math. Methods Appl. Sci. 44 (2021), 13633–13658. https://doi.org/10.1002/mma.7648.

[60] J.M. Cochran, Y. Xu, Age-structured dengue epidemic model, Appl. Anal. 93 (2014), 2249–2276. https://doi.org/10.1080/00036811.2014.918963.

[61] A.K. Supriatna, E. Soewono, S.A. van Gils, A two-age-classes dengue transmission model, Math. Biosci. 216 (2008), 114–121. https://doi.org/10.1016/j.mbs.2008.08.011.

[62] R. Taghikhani, A.B. Gumel, Mathematics of dengue transmission dynamics: Roles of vector vertical transmission and temperature fluctuations, Infect. Dis. Model. 3 (2018), 266–292. https://doi.org/10.1016/j.idm.2018.09.003.

[63] P. Pongsumpun, I.M. Tang, N. Wongvanich, Optimal control of the dengue dynamical transmission with vertical transmission, Adv. Differ. Equ. 2019 (2019), 176. https://doi.org/10.1186/s13662-019-2120-6.

[64] L. Zou, J. Chen, X. Feng, S. Ruan, Analysis of a dengue model with vertical transmission and application to the 2014 Dengue outbreak in Guangdong Province, China, Bull. Math. Biol. 80 (2018), 2633–2651. https://doi.org/10.1007/s11538-018-0480-9.

[65] S. Janreung, W. Chinviriyasit, S. Chinviriyasit, Mathematical evaluation of the role of cross immunity and nonlinear incidence rate on the transmission dynamics of two dengue serotypes, Adv. Differ. Equ. 2020 (2020), 147. https://doi.org/10.1186/s13662-020-02585-1.

[66] Y. Wang, Y. Li, X. Ren, X. Liu, A periodic dengue model with diapause effect and control measures, Appl. Math. Model. 108 (2022), 469–488. https://doi.org/10.1016/j.apm.2022.03.043.

[67] H.S. Rodrigues, M.T.T. Monteiro, D.F.M. Torres, Seasonality effects on dengue: basic reproduction number, sensitivity analysis and optimal control, Math. Methods Appl. Sci. 39 (2014), 4671–4679. https://doi.org/10.1002/mma.3319.

[68] Y. Zhou, D. Xiao, Y. Li, Bifurcations of an epidemic model with non-monotonic incidence rate of saturated mass action, Chaos Solitons Fractals. 32 (2007), 1903–1915. https://doi.org/10.1016/j.chaos.2006.01.002.

[69] Y. Muroya, Y. Enatsu, Y. Nakata, Global stability of a delayed SIRS epidemic model with a non-monotonic incidence rate, J. Math. Anal. Appl. 377 (2011), 1–14. https://doi.org/10.1016/j.jmaa.2010.10.010.

[70] N. Anggriani, H. Tasman, M.Z. Ndii, et al. The effect of reinfection with the same serotype on dengue transmission dynamics, Appl. Math. Comput. 349 (2019), 62–80. https://doi.org/10.1016/j.amc.2018.12.022.

[71] C. Castillo-Chavez, Z. Feng, W. Huang, On the computation of R_0 and its role on global stability, in: C. Castillo-Chavez, S. Blower, P. Van Den Driessche, D. Kirschner, A.-A. Yakubu (Eds.), Mathematical Approaches for Emerging and Reemerging Infectious Diseases: An Introduction, Springer, New York, 2002: pp. 229–250. https://doi.org/10.1007/978-1-4757-3667-0_13.

[72] C. Castillo-Chavez, B. Song, Dynamical models of tuberculosis and their applications, Math. Biosci. Eng. 1 (2004), 361–404. https://doi.org/10.3934/mbe.2004.1.361.

[73] K. Blayneh, Y. Cao, H.D. Kwon, Optimal control of vector-borne diseases: Treatment and prevention, Discr. Contin. Dyn. Syst. - B. 11 (2009), 587–611. https://doi.org/10.3934/dcdsb.2009.11.587.

[74] M.G.M. Gomes, L.J. White, G.F. Medley, Infection, reinfection, and vaccination under suboptimal immune protection: epidemiological perspectives, J. Theor. Biol. 228 (2004), 539–549. https://doi.org/10.1016/j.jtbi.2004.02.015.

[75] A. Khatua, T.K. Kar, Dynamical behavior and control strategy of a dengue epidemic model, Eur. Phys. J. Plus. 135 (2020), 643. https://doi.org/10.1140/epjp/s13360-020-00654-8.

[76] Centers for Disease Control and Prevention, https://www.cdc.gov/dengue/symptoms/index.html. Accessed: December 20, 2022.

[77] P.L. Summers, K.H. Eckels, J.M. Dalrymple, et al. Antibody response to dengue-2 vaccine measured by two different radioimmunoassay methods, J. Clin. Microbiol. 19 (1984), 651–659. https://doi.org/10.1128/jcm.19.5.651-659.1984.

[78] Centers for Disease Control and Prevention, https://www.cdc.gov/malaria/about/biology/index.html. Accessed: December 16, 2022.